PHREEQC Modeling of molybdenum in the Botlek area

Master's thesis

Daniël van Benthem

19-12-2015

PHREEQC Modeling of molybdenum in the Botlek area

Applying the geochemical modeling program PHREEQC to investigate the behaviour of molybdenum in the subsurface of the Botlek area.

Master's thesis

Daniël van Benthem

19-12-2015

Supervisors

Dr. Amir Raoof	Utrecht University
Prof. Dr. Ruud Schotting	Utrecht University
Dr. Annemieke Marsman	Deltares
Bas van der Grift	Deltares

Utrecht University
Faculty of Geosciences
Department of Earth Sciences
Section of Environmental Hydrogeology

Deltares
Enabling Delta Life

Universiteit Utrecht

Acknowledgements

I would like to thank all the people who have supported me in this research project and who made this report possible. First of all, my special thanks go to Annemieke Marsman of Deltares for giving me the opportunity to do my master's thesis at Deltares, providing me with an interesting topic and giving me the support during the time I spent here, and Bas van der Grift of Deltares, for all the detailed help on geochemistry and Phreeqc in particular.
Furthermore I'd like to thank Pauline Gaans of Deltares, and Niels Hartog, Amir Raoof and Thilo Behrends, all of the University Utrecht, for their input and comments during the past months.
Last but not least, Marvin, Joeri, Roy, thank you all for the feedback, conversations and discussions we had during the last months.

Abstract

The Botlek in the Port of Rotterdam contains molybdenum contaminations exceeding the intervention value. Because little is known about the geochemical behaviour of molybdenum in the subsurface, a study consisting of a part literature review and a part geochemical modeling with the program PHREEQC was done. Based on measurements from the field, and the information available from literature, PHEEQC was used to determine the speciation, degree of adsorption, and precipitation reactions that control molybdenum concentrations and transport in the subsurface. In addition, the possibility of making time scenarios for future contamination development was investigated.
The conclusion of this study is that the fate of molybdenum in the subsurface is determined by three processes: the precipitation of molybdenite, the precipitation of iron molybdate, and the adsorption of molybdate on iron oxyhydroxides in the subsurface.
However, as essential information about the kinetics of the precipitation reactions is missing, no further conclusions regarding time and extent of these precipitation reactions can be done. Adsorption does occur, but values determining the degree of adsorption are taken from literature and not from data from the Botlek itself.
Based on this study, a table of recommended measurements is made to do further research on the kinetics of these precipitation reactions, and measure the subsurface of the Botlek for a better insight in the groundwater composition and to obtain more information about the subsurface, its constituents and its relationship with adsorption.

Table of Contents

List of figures

List of tables

Glossary

1. Elements, speciation and minerals

Molybdenum = Mo
Tungsten = W
Chromium = Cr
Vanadium = V
Nitrogen = N
Iron = Fe
Sulphur = S
Manganese = Mn
Ferric iron = Fe^{3+}
Ferrous iron = Fe^{2+}
Calcium = Ca
Natrium = Na
Oxygen = O_2
Molybdate = MoO_4^{2-}
Sulphate = SO_4^{2-}
Phosphate = PO_4^{3-}
Silicate = SiO_4^{4-}
Nitrate = NO_3^-
Calcium carbonate = $CaCO_3$
Iron(II)molybdate = $FeMoO_4$
Molybdenite = MoS_2
Jordisite = MoS_2
Wulfenite = $PbMoO_4$
Ferrimolybdate = $FeMo_3O_{12}{\cdot}8H_2O$
Powellite = $CaMoO_4$
Tetrathiomolybdate = MoS_4^{2-}
Pyrite = FeS_2
Mackinawite = FeS
Sulphur dioxide = SO_2
Molybdenum oxide = MoO
Ammoniumdimolybdate = $((NH_4)_2Mo_2O_7)$
Molybdenum trioxide = MoO_3
Sulphuric acid = H_2SO_4
Organic matter = CH_2O
Carbon monoxide = CO
Carbon dioxide = CO_2
Cyclopentadiene = C_5H_6
Nitric oxide = NO
Halogen elements = F, Cl, Br, I, At
Dithionite = $S_2O_4^{2-}$
Hepta, -octamolybdate = $Mo_8O_{26}^{4-}$, $Mo_7O_{24}^{6-}$
Protonated molybdate = $HMoO_4^-$, H_2MoO_4, $HMo_7O_{24}^{5-}$, $H_2Mo_7O_{24}^{4-}$
Sodium molybdate = Na_2MoO_4
Kaolinite = $(Al_2Si_2O_5(OH)_4)$
Montmorillonite = $((Na,Ca)0,3(Al,Mg)_2Si_4O_{10}(OH)_2{\cdot}n)$

Illite = ((K,H3O)(Al,Mg,Fe)2(Si,Al)4O10[(OH)2,(H2O)])
Tetrathiomolybdate = MoS_4^{2-}
Goethite = a-FeOOH
Ferrihydrite = FeOOH

2. Parameters transport

C = concentration in water (mol/kgw)
t = time (s)
v = pore flow velocity (m/s)
x = distance (m)
D_L = hydrodynamic dispersion coefficient (m^2/s)
$D_L = D_e + \alpha_L v$
D_e = effective diffusion coefficient (m^2/s)
α_L = dispersivity (m)
q = concentration in solid phase (mol/kgw in the pores)

3. Parameters adsorption and surface hydroxyl groups

K_{app} = Adsorption equilibrium constant
K_{intr} = Intrinsic constant
K_{coul} = Coulomb constant
DDL = diffuse double layer model
≡SOH = surface hydroxyl groups
ΔZ = change in the charge of the ion
F = Faraday's constant in Coulombs/mol
R = gas constant in 8.314 J/mol/K
T = absolute temperature in K
Ψ_0 = surface potential in V
σ = surface charge density in Coulombs/m^2
I = ionic strength in mol/L
z = valence of a symmetrical background electrolyte
$[\equiv SOH]_{tot}$ = total concentration of surface sites per volume solution
A_s = Specific surface area in m^2/g
c = particle concentration in g/L
N_S = surface site density in sites/nm^2
N_A = Avogadro's number ($6.0221413 * 10^{23}$ sites/mol)

4. Solubility

SI = saturation index
IAP = ion activity product
K = solubility product

1.

Introduction

1.1 Mega-site approach of the Port of Rotterdam

The Port of Rotterdam deals with soil and groundwater pollution on a very large scale. The port can be divided in different areas with each area containing industrial activities potentially causing a lot of soil and groundwater pollution, e.g. petrochemical industries, refineries, chemical processing industries.
Deltares participates in the research of a joint mega-site approach for the Port of Rotterdam: multiple companies cooperate to deal with the pollution situation throughout the whole port. Rather than approaching contaminations in the traditional manner (i.e. indicate sources of pollution and remediate the pollution), the mega-site approach goes about it differently. In this mega-site approach it is determined which sources form a possible threat for passing a precautionary border and subsequent soil use and the quality of ground and surface water, and need to be dealt with. Because of the biodegradation of many pollutants over time, they will not pass this border. Therefore, not every source needs to be addressed. This approach has the advantages of being cost-effective and in need of less monitoring, and less actual measures need to be taken. Furthermore, in this way the capacity of the soil to remediate are optimally utilised, as a lot of the contaminants are degraded in the soil over time, leading to a more manageable site altogether.
The majority of contaminants are BTEX and VOC's, DNAPLS, which are biodegradable. One pollutant is the transition metal molybdenum (Mo). As a metal, molybdenum will not degrade. It can however, adsorb to minerals in the subsurface, retarding its transport. This process will not stop the transport of molybdenum: eventually it will flow through the subsurface. Furthermore, molybdenum can react with other chemical constituents in the soil and subsequently precipitate.
The Botlek is a part of the Port of Rotterdam located in the middle of the entire port. It was intended to be build and installed at the end of the forties. Due to obstructions and delays, it wasn't before 1955 they started constructing the terrain, and in 1960 it was finished. Since then, the Port of Rotterdam has been constructing more terrain to the west, where the harbour meets the North Sea. The sources of pollution in the in the subsurface follow the chronological order of the constructions in the. As we go west in the harbour, the facilities have been constructed in later years, when attention for environmental concerns became more apparent. Therefore, more to the west the industrial complexes that have been constructed have stricter rules regarding pollution to govern to. In the Botlek however, production processes started in the sixties, when there was less known about the harmful effects of industrial activities on the environment. In the eastern part of the Botlek, Climax and Lyondell are situated.
Globally, the subsurface of the Botlek can be divided in four important layers:

1) Anthropogenic upper sandy/silt layer

2) Holocene sand layer, with intermediate clay layers

3) Holocene clay layer

4) Pleistocene aquifer

the contaminants are introduced into the ground where they dissolve in the groundwater and are transferred as solutions in the subsurface. A study by Deltares (2012) has indicated molybdenum in the subsurface of the Botlek can be found as the oxyanion molybdate (MoO_4^{2-}).
If the molybdenum contamination reaches the aquifer below the clay layer, it will, in theory, be

transported by the water through this sand layer and pass the precautionary border.
The site in the Botlek that has molybdenum contamination has been under research for some time. Measurements have been done on the concentration of molybdenum in different measurement wells. With iMOD, flow models of the area have also been made, showing the progression of the contamination in the groundwater. iMOD is a special graphical user interface and includes an accelerated version of MODFLOW, with the subsurface model GeoTOP of TNO. A more detailed description about iMOD and MODFLOW will be given in the chapter methods.

1.2 Molybdenum

The mineral molybdenite (MoS_2) is processed by Climax and Lyondell to molybdenum which is used in all sorts of industrial applications. Molybdenite itself is highly insoluble in water (Ryzhenko, 2008) and it is likely it oxidized to molybdate and got introduced to the groundwater. Due to improper infrastructure on the terrain, infiltration into the subsurface was not prohibited in any way (Bk Bodem, 2012a). Molybdenum might form a risk for the boundary of the harbour. The behaviour of molybdenum in the subsurface is unknown. It is not clear how molybdenum or molybdate spreads through the aquifer towards the boundary of the port with time. PHREEQC (Parkhurst and Appelo, 2005) is a program that can calculate a variety of chemical reactions and make transport measurements in a 1D column. Given a set of input parameters, and describing the method of transport, one can make a model that would give a clear view of what would happen to a contamination in the subsurface.
As mentioned before, the source of contamination is somewhat disputed. It could be spillage of the source material, leakage of the (by) products or the disposal of waste. Either way, it is determined that molybdenum got introduced to the subsurface by rainwater. The start of the contamination is assumed to be when the facilities of Climax and Lyondell started their operations. For Climax, this would be the year 1966. For Lyondell, this would be the year 1972.
An important part of the research is to determine the speciation and transport of molybdenum in the sand and clay layers, and the influence of other minerals and chemical constituents in the subsurface.

1.3 Research question

The geochemical behaviour of molybdenum in the subsurface in the Port of Rotterdam is not well known. A large amount of molybdenum has infiltrated in the subsurface, and due to a very slow groundwater velocity in the Holocene layers, molybdenum moves very slow. Statements have been made about molybdenum accumulating at the top of a clay layer separating the aquifer below from the contamination. However, measurements show molybdenum amounts far exceeding the intervention value, in the aquifer below this clay layer. It is therefore unknown what is actually happening with molybdenum at the clay layer. Because the polders surrounding the harbour area have environmental restrictions, contaminations from the harbour are not allowed to travel past the boarder. For a more detailed description of molybdenum behaviour in the subsurface, a specific research has to be conducted.
Using the geochemical modelling program PHREEQC the subsurface groundwater constituents can be modelled in a 1D column that shows the interactions between an aqueous solution and the subsurface. Speciation, surface complexation and redox reactions can all be modelled using this program. Geochemical parameters will be made available from field measurements in the Botlek area.
Earlier research (BK Bodem 2012a; Bk Bodem 2012b; Deltares, 2012) suggests that molybdenum will be the (mobile) specie molybdate under the conditions of the Botlek. Possible precipitation could occur in the form of molybdenite and iron molybdate ($FeMoO_4$), or other anions bonded to molybdenum. It is suggested that adsorption of molybdate on iron or aluminium oxides, or clay particles, is also happening. The amount of adsorbed molybdate and the tendency of molybdate to adsorb such minerals however, are both not clear.
With input and parameters and information about the transport at the Botlek, the intention is to make a

PHREEQC model that can describe the complexation of molybdenum that takes place, the amount of adsorption, and the possible precipitation reactions it can form. With this information, statements about the spreading into the aquifer can be made. A sensitivity analysis can then be done to measure the influence of different factors. For example the effects of pH and other ions in the solution can be investigated. Different theories suggesting the precipitation of molybdenum with another ion could be tested in this way. Also, the role of the clay layer in the subsurface in relation with the contamination can be examined and a conclusion can possibly be drawn about the retention of the contamination to the aquifer below.

1.4 Layout thesis

In detail, I will describe the geographical and geological situation of the industrial complexes of Climax and Lyondell. The production processes of both companies will be highlighted as well as the possible origins of contamination.
My report will include a literature research about molybdenum, its speciation, geochemical behaviour and chemical properties. A short review about the mechanics and chemistry of (molybdenum) adsorption and the transport of molybdenum will be given. Furthermore, a description of possible reactions of molybdenum in the subsurface with the other ions in solution needs to be given as well. For the modelling, I will include a description of how the program PHREEQC works and the necessary input information needed for the model.
The input for PHREEQC consists of groundwater chemistry measurements as well as molybdenum measurements from the field. These measurements will be assigned to a well, which has coordinates and a depth. These wells can be found on a map of the area; in this way, the measurements coming from the areas with the (predicted) highest level of contamination can then be modelled in PHREEQC. These highest measurements give us an indication of the maximum level of risk. In a 1D column, we can measure the time needed for the contamination in the top to reach the aquifer. Based on the results of the model, in a conclusion I will present an answer to the research question, after which I will discuss the results and answer of my research question in the discussion section.

2.

Theory

2.1 Situation of the Botlek

Figure 1 below shows the area of the Botlek, surrounded by the blue border. The picture was taken from Google Earth, and it clearly shows the location of the Botlek in the Port of Rotterdam, with reference to Rotterdam and the entire Port of Rotterdam. Throughout the years, the port has been constructed from right to left, even including expansions into the North Sea. Pernis was founded in 1950, the Botlek around 1960 and the Europoort was constructed from 1970 until 1980. The Maasvlakte was taken in use in the seventies, and the second Maasvlakte in the twenty-tens.

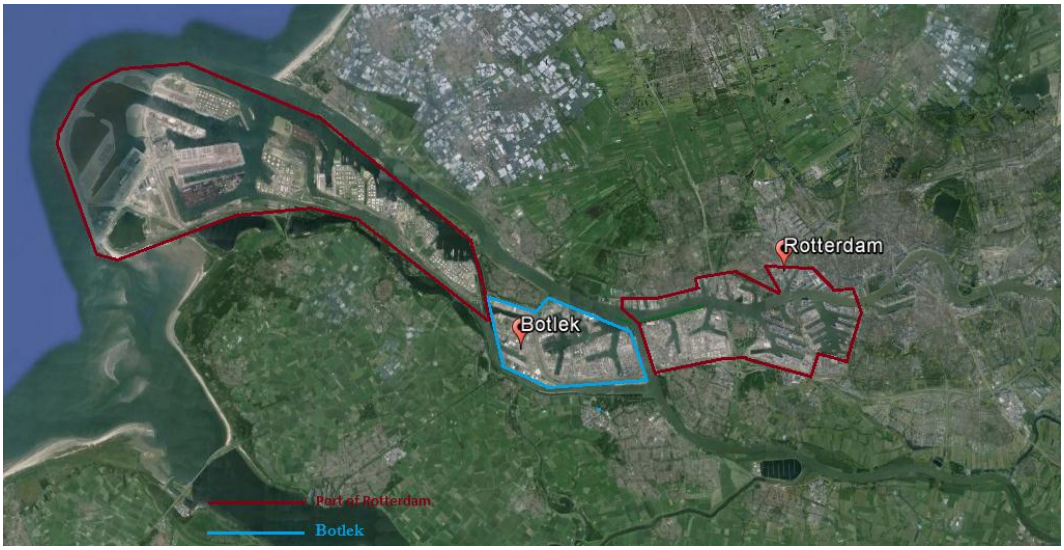

Figure 1: Area Port of Rotterdam and the Botlek

Figure 2 below shows geographical area of the site in the Botlek. Climax Molybdenum B.V. and Lyondell Chemie Nederland are depicted in the figure in the red area and yellow area respectively.

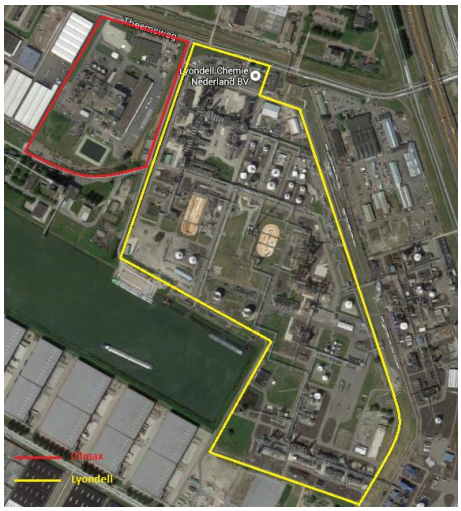

Figure 2: Area Climax and Lyondell

Figure 3 below is obtained from iMOD and shows a rough division of the layers of the subsurface at the Botlek, to get an impression of the geology.

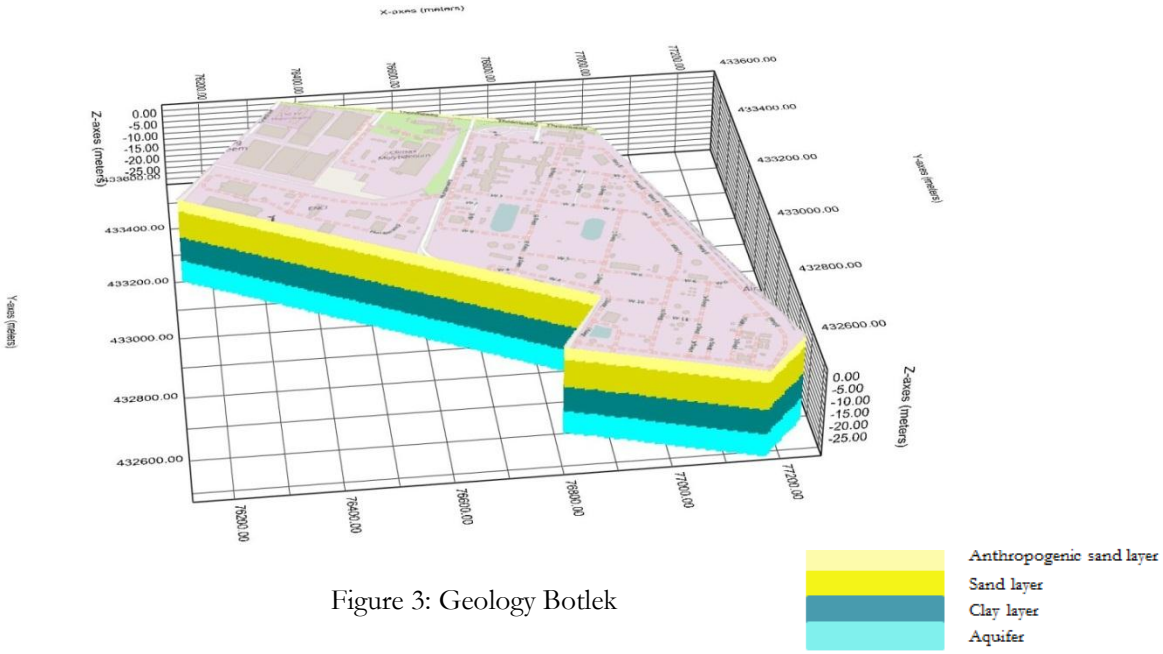

Figure 3: Geology Botlek

Four distinct layers can be seen in figure 3. The top layer is a sand layer, of which the top 5 meters have an anthropogenic origin. It is followed by a clay layer, which is situated above the aquifer that is connected to the polders surrounding the Port of Rotterdam.

2.2.1 Area Climax Molybdenum B.V.

The total area of the Climax site is approximately 70000 m². The next facilities are part of Climax:

1) A roast plant, in use since 1966.

2) A chemical plant, ammonium-dimolybdate or ADM plant, in use since 1972.

3) A flue gas purification plant (sulphuric acid plant), in use since 1981. Before that, sulphur dioxide (SO_2) was emitted into the atmosphere by a chimney situated on the terrain.

2.2.2 Production processes Climax

In the roast plant, molybdenite is oxidized to produce molybdenum oxide (MoO). Next, in the ADM plant, from this molybdenum oxide, ammoniumdimolybdate ($(NH_4)_2Mo_2O_7$) and molybdenum trioxide (MoO_3) are produced. The reactions in the roast plant take place under temperatures of 500 – 650 ℃. The overall reactions of producing molybdenum trioxide from molybdenite can be given by (IMOA, 1989):

$$2\ MoS_2 + 7\ O_2 \rightarrow 2\ MoO_3 + 4\ SO_2 \quad (2.1)$$
$$MoS_2 + 6\ MoO_3 \rightarrow 7\ MoO_2 + 2\ SO_2 \quad (2.2)$$
$$2\ MoO_2 + O_2 \rightarrow 2\ MoO_3 \quad (2.3)$$

The reaction of molybdenum oxide forming ammoniumdimolybdate is given by (IMOA, 1989):

$$2\ O_2 + H_2O + 2\ NH_3\ (aq) + 2\ MoO \rightarrow (NH_4)_2Mo_2O_7 \quad (2.4)$$

And the reaction forming molybdenum trioxide from molybdenum oxide (IMOA, 1989):

$$MoO + 0_2 \rightarrow MoO_3 \quad (2.5)$$

The flue gas purification plant then produces sulphuric acid (H_2SO_4) from sulphur dioxide which is a rest product from the production of molybdenum oxide (Stumm and Morgan, 1996):

$$2\ SO_2 + 2\ H_2O + O_2 \rightarrow 2\ H_2SO_4 \quad (2.6)$$

It is not mentioned in the reports of Bk Bodem (2012a, 2012b), Deltares (2012), MWH (2014) whether and how in these processes waste was deposited as Climax did not report this. Measurements however (Bk Bodem, 2012a; MWH, 2014) clearly show a large amount of molybdate and sulphate in the subsurface, still in the anthropogenic layer. This could be the result of oxidation of molybdenite on the surface of the terrain, and subsequent infiltration in the subsurface by rainwater precipitation.

2.2.3 Origin of contamination

Information about the origin of the molybdenum contamination is unclear. According to BK Bodem (2012a), the main source of the contamination is due to spillage of raw molybdenite on the ground, sometime after production processes began in 1966. Another contribution would be through deposition by rainfall of molybdenum that has been emitted to air, but this is considered to be an implausible scenario. Strong winds from the North Sea would not allow emission of molybdenum to be deposited on the same place as where it was emitted into the atmosphere. But if the first scenario is the case; than this would implicate molybdenite would enter the subsurface through infiltration by rainwater. In 2006, a 'black-topping' (asphalt) was deployed on the entire site; which prevents rainwater to infiltrate in the subsurface and supplement the groundwater. The contaminated rainwater is caught and treated since 2006 at the waste water treatment plant on the southern part of the site. There is no more additional contamination since this black-topping has been installed. As infiltrations rates are also lowered by this black-topping, the entire transport of molybdenum in the subsurface occurs at a slower pace. Furthermore it is concluded that the contamination is legally regarded as 'historically'; meaning the majority of the contamination originates from the period 1965-1987 (Bk Bodem, 2012a).
Measurements done by UT2A provide an amount of molybdate in µg Mo/L. Of these measurements, 2 are taken on the area of Lyondell, and the other 4 on the area of Climax. The measurements on the Lyondell area were taken from the aquifer.
Measurements done by MWH Global indicate a high amount of sulphate in the anthropogenic top layer (200-300 centimetres below the ground level). Values of up to 400 mg/L sulphate at some locations, combined with the high amounts of molybdate in the top layer (values up to 17 mg/L) suggest that the raw molybdenite gets oxidized by oxygen under influence of rainwater and got introduced to the subsurface.

$$MoS_2 + 9\ O_2 + 12\ H^+ \rightarrow MoO_4^{-2} + 2\ SO_4^{2-} + 6\ H_2O \quad (2.7)$$

Other oxidation reactions of molybdenite are given by Bellantoni (2014):

$$MoS_2 + 10\ H_2O \rightarrow MoO_2^{+} + 2\ SO_4^{2-} + 20\ H^+ + 17\ e^- \quad (2.8)$$
$$MoS_2 + 12\ H_2O \rightarrow MoO_4^{2-} + 2\ SO_4^{2-} + 24\ H^+ + 18\ e^- \quad (2.9)$$

2.2.4 Contamination measurements 2012

Figure 4 below shows the area of Climax and a part of Lyondell, but focuses only on Climax.

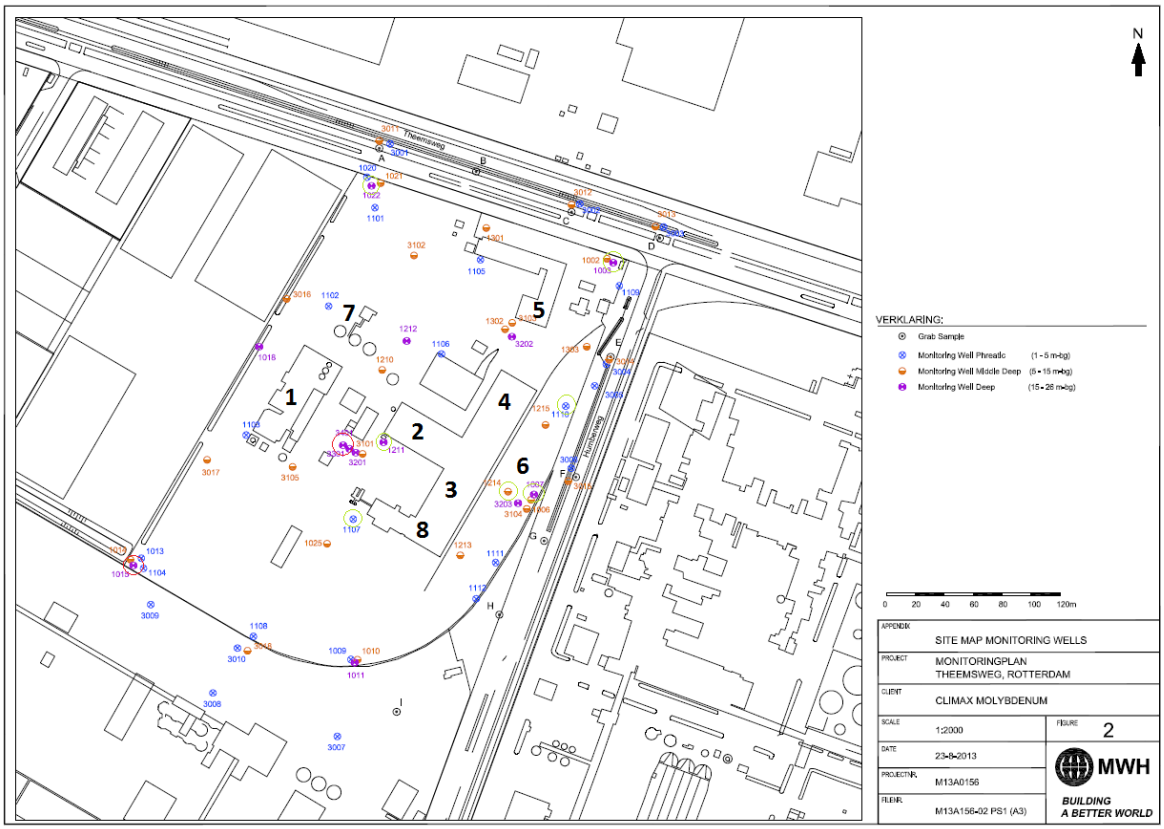

Figure 4: Climax facilities with measurement wells

The red circles indicate the measurement wells that were used by UT2A, and the green circles indicate the wells with the values over the intervention values as measured by Bk Bodem (2012b).

1 = Flue gas purification plant
2 = Roast plant
3 = Warehouse
4 = Warehouse
5 = Office building
6 = Outside storage facility
7 = Storage
8 = ADM plant

Earlier groundwater measurements done by BK Bodem (2012a) indicate two core areas with severe contamination:

1) Around the roast installation, the AMD plant and storage.

2) The area around the Flue gas purification plant.

The contamination of molybdenum can be divided in three categories: target value (light contamination), intervention value (strong contamination) and intermediate value (medium contamination). The target

value and intervention value are self-explanatory; the intermediate value is a value calculated by Bk Bodem (2012a): (target value + intervention value)/2 and smaller than or equal to the intervention value.

Table 1. Contamination guideline values

Target value (S)	Intermediate value (T)	Intervention value (I)
5 µg/l	153 µg/l	300 µg/l

Measurements by Bk Bodem (2012b) indicate that, especially in the anthropogenic sand layer, the measured molybdenum values exceed the intervention values plenty: values as much as 197 times the intervention value have been monitored. The values at measurement wells 1107 and 1110 are extremely high: these are near the warehouse.
In the sand layer below, values above the intervention values are a little less common. Still, values exceed this value with a factor 50. Especially around wells 1214 and 1215, again, located near the warehouse, values are very high.
In the aquifer, values do exceed the target value, but not the intermediate value or the intervention value. The exceptional high value is this time, also at the cluster where the other values are also very high: on the terrain right of the warehouse. Other values are scattered around the entire site.
The measurements by UT2A (2014) indicate values high above the target value but not above the intervention value, these are located in the wells 1015 and 3401 which are in the far South-West and middle of the terrain, respectively.

2.2.5 Hydrogeology and subsurface geology

For the hydrogeology iMOD was used to take a cross-section of the layers that constitute the geology of the Botlek.
For both Climax and Lyondell a section was taken. The profile depicts the vertical transmissivity and gives a clear distinction between the sand and clay layers. In iMOD, layers containing information about transmissivity were loaded up to a depth of 45 meters. The distinction was made at 0.01 m/day as this gives a clear distinction between sand and clay layers which gives us an accurate overview of the subsurface. Values below 0.01 m/day were identified as clay layers, values above 0.01 m/day were sand layers. The cross-section for the area containing the Climax industry (figure 5):

Table 2. Geology Climax

Depth (m)	Hydrogeological unit	Lithography
+5.02 : -10.97	Artificial layer, sand layer	Sand (Holocene)
-10.97 : -20.95	Clay layer	Clay
-20.95 : -38.98	Aquifer	Sand (Pleistocene)
-38.98 : -39.94	Clay layer	Clay
-39.94 >	Sand layer	Sand

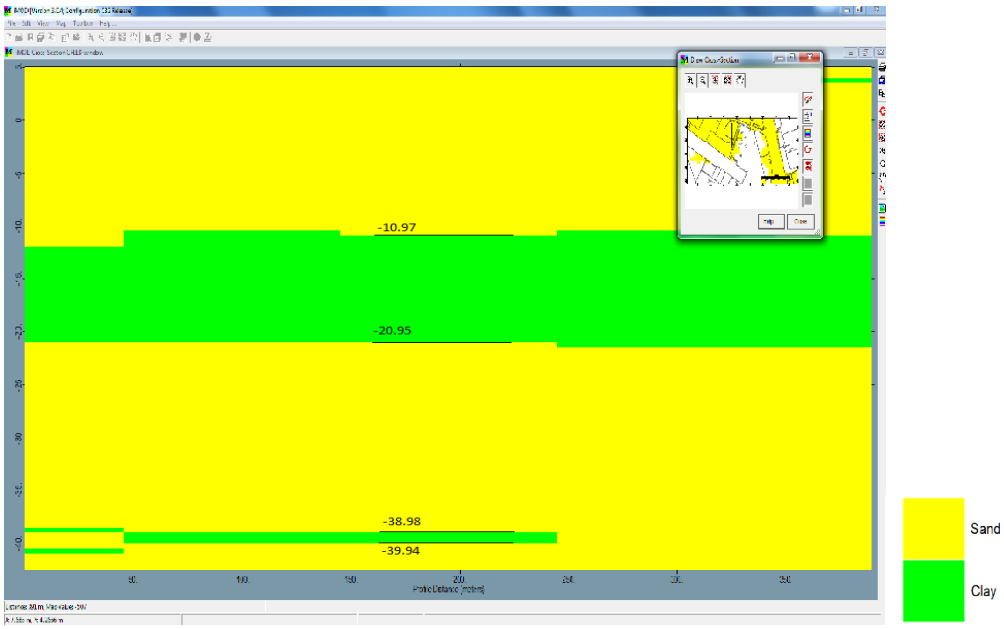

Figure 5: section geology Climax

2.3.1 Lyondell Chemie Nederland B.V.

Due to lacking information about groundwater samples from the Lyondell area, this research is mainly focused on Climax. However, the area of Lyondell does contain elevated concentrations of molybdate in the subsurface, and therefore a brief review concerning the situation of Lyondell will be given.
Lyondell Chemie Nederland B.V. has a site-area lager than Climax. Its midpoint is located – according to the topographical map of the Netherlands- on the coordinates: x = 76953, y = 433368. The terrain of Lyondell is surrounded by the Humberweg on the Westside, the Theemsweg on the north side and the Seinehaven on the south. Lyondell was established in 1972 as Oxirane chemie; and uses a multitude of chemical substances in its processes, of which molybdenum is one such chemical substance. Molybdenum trioxide is predominantly used as a katalysator in the production of synthetic materials and chemical semi-finished products. The site that's part of Lyondell has a significant contamination in the north-western part. This contamination could be the result of molybdenum trioxide coming in contact with rainwater (IMOA, 1989; Allison et al., 1991):

$$MoO_3 + H_2O \rightarrow MoO_4^{-2} + 2\,H^+ \qquad (2.10)$$

2.3.2 Hydrogeology and subsurface geology

The profile on the next page depicts the cross-section of the area where Lyondell is situated (figure 6). The distinction of the layers is:

Table 3. Geology Lyondell

Depth (m)	Hydrogeological unit	Lithography
+5.02 : -12.98	Artificial layer, sand layer	Sand (Holocene)
-12.98 : -14.45	Clay layer	Clay
-14.45 : -15.52	Sand layer	Sand
-15.52 : -15.92	Clay layer	Clay
-15.92 : -16.99	Sand layer	Sand
-16.99 : -17.95	Clay layer	Clay
-17.95 : -19.03	Sand layer	Sand
-19.03 : -19.93	Clay layer	Clay
-19.93 : -20.44	Sand layer	Sand
-20.44 : -20.95	Clay layer	Clay
-20.95 : -37.00	Aquifer	Sand (Pleistocene)
-37.00 : -37.45	Clay layer	Clay
-37.45 : -38.02	Sand layer	Sand
-38.02 : -39.94	Clay layer	Clay
-39.94 >	Sand layer	Sand

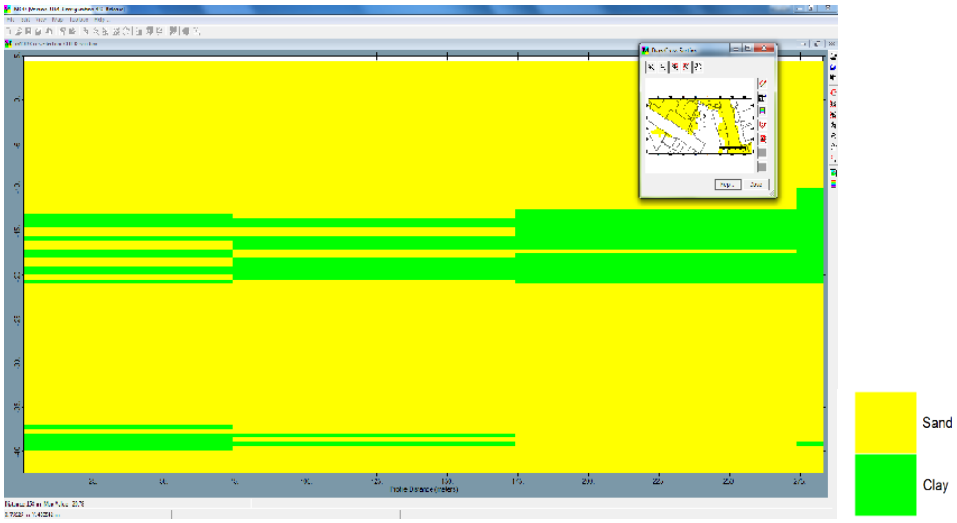

Figure 6: section geology Lyondell

2.4 Contamination plume

The contamination of molybdenum in 2014 has spread across the entire industrial area of Climax with the high levels of contamination in the north-eastern area. It spreads southwards to the Seinehave in relative high concentrations. An amount is also located at the industrial area of Lyondell, in the north-west of the Lyondell area. These concentrations are a little less high as at Climax, but still higher than the intervention value.

In the aquifer, values above the intervention value have also been detected, mostly surrounding the North-Eastern area of Climax and the north-western area of Lyondell. Furthermore, traces of molybdenum above the target value and above the intermediate and intervention can also be found scattered across the area of Climax, albeit less abundant (still).

2.5 Molybdenum

Molybdenum (Mo) is a chemical element with atomic number 42 and an atomic mass of 96 u. It is the fourth member of the second transition series and is located in group 6 in the periodic table, together with tungsten (W) and chromium (Cr). It is a transition metal with a very high melting point (sixth highest of all metals on earth), with chemical properties that resemble tungsten and vanadium (V). Molybdenum is strongly chalcophile or siderophile (i.e. prefers to react with sulphur or iron), and can normally be found in nature in the minerals molybdenite, wulfenite ($PbMoO_4$), ferrimolybdate ($FeMo_3O_{12}\cdot 8H_2O$), iron(II)molybdate, jordisite and powellite ($CaMoO_4$). In the literature it is not clearly stated what the difference is between molybdenite and jordisite, both MoS_2, but in the remainder of this report molybdenite is taken as the mineral representing MoS_2. Commercially, molybdenum is obtained by mining molybdenite. It is an essential trace element in the biosphere as it catalyses redox reactions in plants and animals and is beneficial to human health as well.
Molybdenum forms compounds in a wide range of interconvertible oxidation states (paragraph below will describe this in detail), complexes with organic and inorganic ligands including physiologically important compounds, and binuclear and polynuclear species which involve bridging ligands such as oxide, hydroxide and sulphide or metal-metal bonds between molybdenum atoms. Compounds in which the molybdenum coordination number ranges from 4 to 8 can also be found (IMOA, 2015).
Popular compounds include molybdenum trioxide and molybdenum-oxygen compounds; these are added to alloys (to increase strength, temperature strength, durability etc.) and other industrial applications, and molybdenum-sulphur compounds, commonly used for lubrication to reduce friction and increase durability (comparable to graphite). Additionally, molybdenum is also added to fertilizer, to prevent molybdenum deficiency in plants and crops, and is widely applied in the electronics industry (Xu et al., 2013).
The common method of contamination of molybdenum is from molybdenum compounds coming from industrial activities that are released in the environment through emission, wastewater and solid waste (sludge) (IMOA, 2015). Guidelines established by the WHO (2011), cite 0.07 mg/L as the maximum daily intake of Mo for humans which is considered safe. This corresponds to 70 µg/L.

2.5.1 Oxidation states

As a compound, molybdenum can occur in oxidation states from –2 to +6. Oxidation states of –2 to +2 are most likely not encountered in biological systems or an enzymatic process and we can therefore assume they will not show up in the groundwater samples.
Molybdenum in the oxidation states +3 to +6 commonly binds to oxygen-, sulphur- and nitrogen-donor ligands and with the halogen elements (F, Cl, Br, I, At). Molybdenum with oxidation states +5 and +6 are commonly dominated by species that consist of either one or more oxygen atoms and one or two molybdenum atoms; the oxomolybdenum species (Xu et al., 2013; IMOA, 2015).
Molybdenum (+5) is formed through various forms of reduction, and molybdenum (+6) may be reduced by dithionite ($S_2O_4^{2-}$) to molybdenum (5+) and oxo molybdenum (4+) complexes (MoO^{2-}). Next, we will see the likelihood of the molybdenum oxyanion with the highest oxidation state (+6); molybdate.

2.5.2 Molybdenum speciation in the subsurface

When molybdenum encounters an aqueous solution, it can occur in different species, depending on the pH of the solution and the concentration of molybdenum present.
In oxic and suboxic conditions, with a neutral pH, molybdenum will be encountered mainly as molybdate. Molybdate is a tetrahedral, monomeric molybdenum specie that consist of molybdenum in its highest oxidation state of 6^+ together with four oxygen atoms. Figure 7 below shows the structural configuration of the molybdate ion.

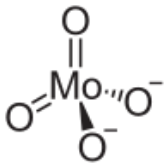

Figure 7: Structural configuration molybdate ion

Often, other examples of molybdenum species such as $(Mo_2O_7)^{2-}$ and $(Mo_3O_{10})^{2-}$ are also called molybdate. Strictly speaking however, these are polynuclear molybdates, but they are referred to as molybdate. Molybdate is the dominant specie at a pH > 6. If pH values drop, the molybdate anion becomes protonated. Polymerisation of molybdate to hepta- or octa- molybdate can happen and depends on pH and concentration of molybdenum. When pH values drop below 4.4 (Xu et al., 2013), the molybdate anion will fully protonate to $MoO_3(H_2O)_3$. An overview of the speciation of molybdenum in aqueous solutions is given in table 4 below:

Table 4. Molybdenum speciation

$[Mo^{6+}]$/mol L^{-1}	**$[Mo^{6+}]$/µg L^{-1}**	**pH**	**Main species**
All	All	>6	MoO_4^{2-}
10^{-5}	959,5	>5	MoO_4^{2-} (ca 100%)
10^{-5}	959,5	4	MoO_4^{2-} (30%), $HMoO_4^-$ or $MoO(OH)_5^-$ (10%), H_2MoO_4 or $Mo(OH)_6$ (60%)
10^{-5}	959,5	2-3	H_2MoO_4 or $Mo(OH)_6$ (ca 100%)
10^{-5}	959,5	1	H_2MoO_4 or $Mo(OH)_6$ (80%), $H_3MoO_4^+$ or $Mo(OH)_5(H_2O)^+$ (20%)
$< 10^{-3}$	95950	>1	Monomeric species only
$> 10^{-3}$	95950	5-6	$Mo_7O_{24}^{6-}$, $HMo_7O_{24}^{5-}$, $H_2Mo_7O_{24}^{4-}$
$> 10^{-3}$	95950	4-5	$Mo_8O_{26}^{4-}$

IMOA (2015)

The protonation and other chemical reactions of molybdate are given in table 5 below:

Table 5. Chemical reactions molybdate

Chemical reactions of molybdate in aqueous solutions
$MoO_4^{2-} + H^+ = HMoO_4^-$
$MoO_4^{2-} + H^+ = MoO_3(H_2O)_3(aq)$
$6\ MoO_4^{2-} + 8\ H^+ = H_2Mo_6O_{21}^{4-} + 3\ H_2O$
$7\ MoO_4^{2-} + 8\ H^+ = Mo_7O_{24}^{6-} + 4\ H_2O$
$7\ MoO_4^{2-} + 9\ H^+ = HMo_7O_{24}^{5-} + 4\ H_2O$
$8\ MoO_4^{2-} + 12\ H^+ = Mo_8O_{26}^{4-} + 6\ H_2O$
$8\ MoO_4^{2-} + 11\ H^+ = H_3Mo_8O_{28}^{5-} + 4\ H_2O$
$MoO_4^{2-} + 2\ H^+ = MoO_3(s) + H_2O$
$MoO_4^{2-} + 2\ H^+ = H_2MoO_4(s)$
$MoO_4^{2-} + 2\ Na^+ = Na_2MoO_4(s)$
$MoO_4^{2-} + 2\ Na^+ + 2\ H_2O = Na_2MoO_4{\cdot}2H_2O(s)$
$2\ MoO_4^{2-} + 2\ Na^+ + 2\ H^+ = Na_2Mo_2O_7(s) + H_2O$

Xu et al. (2013)

2.6 Adsorption of molybdate

Adsorption is an important factor in the transport of contaminants in the subsurface. When a particle gets adsorbed to the subsurface it is located in, it effectively becomes immobile. As such, species of molybdate can become immobile through adsorption. Because of the heterogenetic geology of the Botlek, it is important to know when adsorption occurs, if it applies to the specific area and how it affects the transport of the contaminant. Measurements (MWH, 2014; UT2A, 2014) and the given review in paragraph 1 indicate that molybdate is the main specie present in the subsurface at biological conditions. It is essential however, to obtain good information about the possible adsorbents and the relationship with molybdate.

2.6.1 Adsorption on soils

Adsorption of molybdate on clay minerals, calcium carbonate ($CaCO_3$), aluminium and iron oxide minerals, calcareous and noncalcareous minerals has been studied.
Adsorption behaviour of molybdate on amorphous aluminium and iron oxide minerals, clay minerals, and non-calcareous soils appears to be strongly pH dependent. On aluminium and iron oxide minerals, molybdate adsorbs more easily at pH values 4-5. Above a pH of 5, adsorption decreases and above a pH of 8, adsorption barely occurs. Adsorption on clay minerals also occurs at low pH values; with a peak rate at a pH of 3, after which it rapidly decreases until adsorption is basically zero at a pH of 7.
Adsorption on noncalcareous soils of molybdate peaks between pH 3-4, decreases with increasing pH to 7, and is very low above pH 7 (Stollenwerk, 1995; Goldberg et al., 1996; Goldberg and Forster, 1998; Xu et al., 2005; Rietstra en Harmsen, 2005).
On calcareous soils and calcite, adsorption doesn't play a significant role. Adsorption of oxy anions on soil is pH dependant, and less adsorption takes place at high pH values which is the case with these types of soils (Goldberg et al., 1996).

2.6.2 Adsorption competing anions

Another factor mentioned in literature that influences the degree of adsorption of molybdate is the amount of competing anions (Barrow, 1974; Stollenwerk, 1995; Goldberg and Forster, 1998; Goldberg, 2010; Xu et al., 2005). The adsorptive behaviour of molybdate and tetrathiomolybdate (MoS_4^{2-}) on pyrite (FeS_2) and goethite (a-FeOOH) was studied in order to determine the effects of competitive anions on adsorption, which were sulphate (SO_4^{2-}), phosphate (PO_4^{3-}) and silicate (SiO_4^{4-}). The adsorption of molybdate and tetrathiomolybdate on pyrite and goethite was Langmuir-type (partitioning between gas phase and adsorbed species as a function of applied pressure) at low pH. The rate of adsorption decreased in the order tetrathiomolybdate /goethite > molybdate /goethite > tetrathiomolybdate /pyrite > molybdate /pyrite. They acknowledge the competing effect of phosphate on the adsorption of molybdate on pyrite and goethite, but determined that silicate only has negligible effect, and sulphate has no competing effect. No evidence was found of studies on other competing anions.
Additionally, the concentration of phosphate plays an important role in this case of competitive adsorption. When saturation of the adsorption of phosphate is achieved, the pyrite and goethite go back to molybdate adsorption, as is suggested by Xu et al. (2005). When phosphate ions are present in the soil, molybdate adsorption is delayed.

2.6.3 Soil salinity

Goldberg (2009) measured the influence of the salinity of the soil on the adsorption rate of molybdate. The findings suggested that in the range of pH of 4-8, the soil salinity does not play a role in molybdenum adsorption. In normal biological settings, where pH is approximately 4-8, the soil salinity does not need to be taken into account when making predictions about molybdate adsorption.

2.7 Precipitation of molybdenum

Molybdenum can be lost from a solution by a precipitation reaction. As we previously mentioned, molybdenum is strongly chalcophile or siderophile, meaning it has a preference for being in sulphur or iron compounds.

2.7.1 Molybdenite

According to Ryzhenko (2008), the accumulation of molybdenum in aqueous solutions is limited in sulphuric environments due to the formation of molybdenite and its low degree of solubility.
A proposed theory for the loss of molybdate from the aqueous solution is the reaction between molybdate and sulphides, forming molybdenite (Chappaz et al., 2008):

$$MoO_4^{2-} + 6\ H^+ + 2\ HS^- + 2\ e^- \rightarrow MoS_2 + 4\ H_2O \qquad (2.11)$$

$$\text{Log } K = -59.27$$

The assumption here made is that organic matter reduces sulphate in the solution, forming sulphides (Stumm and Morgan, 1996):

$$SO_4^{2-} + H^+ + 2\ CH_2O \rightarrow HS^- + 2\ H_2O + 2\ CO_2 \qquad (2.12)$$

$$\text{Log } K = 31.6$$

Molybdate can react with sulphides to form and precipitate molybdenite. According to Ryzhenko (2008), the accumulation of molybdenum in aqueous solutions is limited in sulphuric environments due to the formation of molybdenite and its low degree of solubility.
Figure 6 below shows the stability diagram of Mo-S-O-H at 25°C, clearly showing the division between conditions in which molybdate is present, and the conditions in which molybdenite would form. With the conditions in the subsurface at the Botlek (pH and redox), the formation of molybdenite is a possibility. PHREEQC is the ideal program to investigate these conditions and the likelihood of molybdenite precipitates.

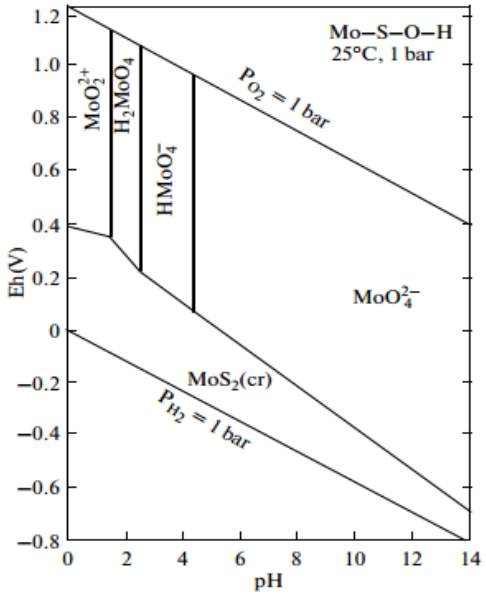

Figure 8: Compositions of molybdenum bearing natural waters in the Eh–pH diagram for the Mo–O–H–S system at 25°C, P = 1 bar. (Ryzhenko, 2008)

2.7.2 Iron(II)molybdate

Another class of precipitates that could form when molybdate is present is iron(II)molybdate. Research by Morrison and Spangler (1992) proposes a theory that molybdate could, under specific conditions, react with ferrous iron to form iron(II) molybdate. This study will also focus on this reaction due to the presence of both molybdate and ferrous iron in the groundwater.
If we look at the stability diagram given below in figure 7, we can see the conditions for the formation of iron(II)molybdate follows the same trend as the formation of molybdenite: at pH values between 6-8, and Eh values between -200 and -300, according to this figure, iron(II)molybdate will form.

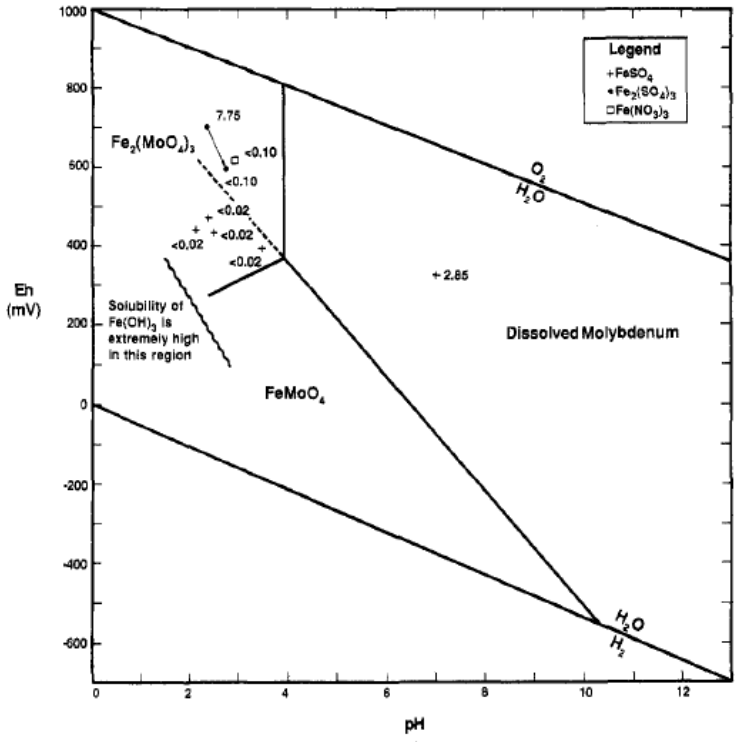

Figure 9: Stability diagram for iron(II)molybdate, at T = 25 ℃, P = 1 bar; in equilibrium with $Fe(OH)_3$; [Mo] = 0.1 mg/L. (Morrison and Spangler, 1992)

2.8 Transport

Transport in porous media is a complex process, involving many aspects one needs to take into account. PHREEQC can model 1D transport, including diffusion, advection and dispersion. The underlying theory is described by the advection-reaction-dispersion equation:

$$\frac{\delta C}{\delta t} = -v\frac{\delta C}{\delta x} - \frac{\delta q}{\delta t} + D_L\frac{\delta^2 C}{\delta x^2} \tag{2.13}$$

The first term represents the advective term, the second term denotes the change in concentration in the solid phase due to reactions and the last term is the dispersive transport.
The effective diffusion coefficient D_e corrects for the extra pathway that needs to be travelled by the solutes when diffusing pore spaces. Diffusion only plays a very small role in the transport of solutes, and especially with rough flow velocities its influence in this particular study can be neglected.
When the front of a solution travels through porous media, it flows around sand grains, resulting in a concentration front that will spread. This is called dispersion. Dispersion can be distinguished in micro and macro dispersion. Furthermore, we can distinguish this micro dispersion in longitudinal dispersion (D_L) and transverse dispersion (D_T). Dispersivity can be linked to dispersion by the flow velocity:

$$\alpha_L = \frac{D_L}{v} \tag{2.14}$$

With α_L as the dispersivity (m).
In turn, the longitudinal dispersion is formed by the dispersivity and the effective diffusion:

$$D_L = D_e + \alpha_L v \tag{2.15}$$

With D_e as the effective diffusion coefficient (m^2/s).
Despite the complexity of the subject, modelling transport in PHREEQC is straightforward. Transport and its components are modelled with the keyword data block TRANSPORT. A number of cells [n] is defined, which are linked to the [n] solutions that are defined in the same model, in the SOLUTION keyword data blocks. Each cell has a cell size that can be individually assigned, or a cluster of cells can be assigned a cell size.
The advective flow is modelled with a shift. Shift moves the solution from one cell to the next, in the direction that you assign with flow-direction. Subsequently, reactions modelled in the model between immobile objects (exchangers, minerals, etc.) and the aqueous solution are performed. The time needed for one shift is determined with a time-step. So, to fill 10 cells with the solution assigned to these cells, one needs at least 10 shifts for the entire body of water to have moved through all cells.
The amount of shifts times time-step is the total simulation time; the length of the cell divided by the time-step is the velocity in that cell. As these velocities differ with depth, one needs to adjust either the cell size or the time-step associated with said depth, so that the velocity or velocities used in PHREEQC are the same as those taken from MODFLOW/MODPATH.

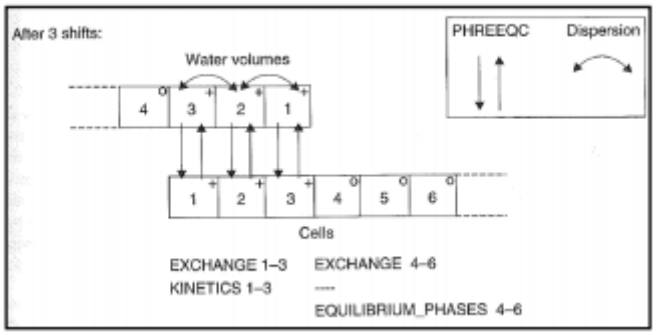

Figure 10: 1D transport process cells in PHREEQC (Appelo and Postma, 2005)

Because of the very low flow velocities in the Botlek, the associated time-steps are very large. One particle track representative for this area in the Botlek was taken and the flow velocities for the entire depth were calculated based on this particle track. With the total depth, the flow velocities at the redox zones, and the total time needed for modelling the contamination (48 years), the amount of cells needed for every redox zone and the time-step associated with the shifts can be determined. For modelling future scenarios, the amount of shifts can be altered to reach the desired total time. Table 6 below show the velocities applied in the PHREEQC model. Because of the vertical flow in the Botlek, the vertical flow velocities were taken for the anthropogenic layer, the sand layer and the clay layer. Using the flow velocities provided by MODFLOW, the vertical component was taken and applied in the PHREEQC model. In the aquifer, the flow is more horizontal, therefore the actual flow velocity obtained from MODFLOW was used.

Table 6: Flow velocities Botlek

Layer	Distance (m)	Depth (m)	Flow velocity (m/s)
Anthropogenic layer	5	+5 : 0	4.8201E-08
Sand layer	5	0 : -5	2.1892E-08
Sand layer	6	-5 : -11	1.9976E-08
Clay layer	9	-11 : -20	2.4027E-08
Aquifer	5	-20 : -25	1.6100E-07

2.8.1 Boundary conditions

The boundary conditions for the first and last cell can be set with the command line boundary-conditions. There are three types of boundary conditions:

1) Constant: concentration is constant, also known as first type or Dirichlet boundary condition. C_0 is the concentration outside the column (mol/kgw).

$$C(x_{end}, t) = C_0 \tag{2.16}$$

2) Closed: no flux at boundary, also known as second type or Neumann boundary condition, with v = 0 as flow velocity (m/s) and

$$\frac{\delta C(x_{end}, t)}{\delta x} = 0 \tag{2.17}$$

3) Flux: flux boundary condition, also known as third type or Cauchy boundary condition, with D_L as the dispersion coefficient:

$$C(x_{end}, t) = C_0 + \frac{D_L}{v}\frac{\delta C(x_{end}, t)}{\delta x} \tag{2.18}$$

For both the first and last cell, the flux boundary condition was applied.

2.9 Redox processes

Redox processes affect the chemical quality of groundwater in all aquifer systems. The groundwater samples taken for measurements in the Botlek are no exclusion. These processes influence the composition of your groundwater sample, remove and produce species in your sample and generally determine the speciation of the element you are trying to model. If one wants to use geochemical parameters in a subsurface contamination model, clearly determining redox processes is of crucial importance.

2.9.1 The redox succession

In natural systems, microorganisms that catalyse redox processes have to compete for limited resources. This competition leads to microorganism favouring the redox processes that generate the maximum amount of available energy. A microbial process that couples the most efficient electron donors to the most efficient electron acceptors has a competitive advantage: the most efficient redox reactions will occur first.
The most common electron donor available in groundwater is often dissolved organic carbon (DOC). Reduced forms of nitrogen (N), iron (Fe), sulphur (S), and possibly other species could also be important electron donors in some cases. Electron acceptors follow the same trend. Dissolved oxygen (O_2) produces the most energy per mole of organic carbon oxidized, and is as such the preferred electron acceptor by subsurface microorganisms. But, groundwater systems are often isolated from the atmosphere, so dissolved oxygen tends to be consumed along aquifer flow paths, making the environment anoxic. Following dissolved oxygen as most energetically favourable naturally available electron acceptor is nitrate (NO_3^-), then manganese (Mn^{4+}), ferric iron (Fe^{3+}), sulphate (SO_4^{2-}) and finally carbon dioxide (CO_2). This order of electron acceptor utilization is termed as the "ecological succession of terminal electron-accepting processes" (McMahon and Chapelle, 2007).
If you take this sequence of electron-accepting processes along a flow path, you can identify which redox processes would take place in a groundwater sample, and based on this sequence, you could make predictions about the species you will find in the groundwater at that depth. McMahon and Chapelle (2007) constructed a framework that should allow the user to assess redox processes in regional aquifer systems. Based on indicator values for essential electron acceptors, a division between redox processes can be made, serving as an indication of redox processes.
This method is not completely flawless; certain limitations can be noted. Concentrations thresholds depend on multiple factors and are therefore variable: microbial species, electron donor availability, and the scale size of sampling all play an important role. For example, it could be that the dissolved oxygen concentration threshold required before the denitrification stage is reached is considered to be around 0.2 to 0.3 mg/L, but it could be in a higher order in some aquifers, even up to 2 mg/L. These larger rates could be the result of multiple flow paths mixing at the sampling at wells. Underestimating these threshold concentrations would lead to an under prediction of the occurrence of a redox process. Applying the framework to regional water quality data will result in a diagnosis pointing to a single redox process. However, in other examples, with aquifer heterogeneities, flow path complexities, and well sample mixing, it is only possible to define multiple 'mixed' redox processes. So, even making general

statements about measurements is rather difficult. Therefore this framework should be seen more as a guideline. Table 7 below shows the threshold concentrations which can help identify the redox processes in the subsurface. When addressing the measurements, this table has been used to compare values of concentrations. It gives some insight in to what kind of process would be happening at that measurements depth.

Table 7. Threshold Concentrations for Identifying Redox processes

Threshold Concentrations for Identifying Redox processes						
	Water Quality Criteria (mg/L)					
Redox Process	**0_2**	**NO_3^-**	**Mn^{2+}**	**Fe^{2+}**	**SO_4^{2-}**	**Comments**
Oxic						
O_2 reduction	≥0.5	-	<0.05	<0.1	-	-
Suboxic					-	
-	<0.5	<0.5	<0.05	<0.1	-	Further definition of redox processes not possible
Anoxic						
NO_3^- reduction	<0.5	≥0.5	<0.05	<0.1	-	-
Mn(IV) reduction	<0.5	<0.5	≥0.5	<0.1	-	-
Fe(III)/SO_4^{2-} reduction	<0.5	<0.5	-	≥0.1	≥0.5	-
Methanogenesis	<0.5	<0.5	-	≥0.1	<0.5	-
Mixed						
-	-	-	-	-	-	Criteria for more than one redox process are met

(McMahon and Chapelle, 2007)

2.10 Adsorption

Ions adsorbed from an aqueous solution accumulate at the surface of a sorbent such as oxide minerals, clay minerals and organic matter. Adsorption onto minerals in the subsurface is particularly important in the PHREEQC model as it influences the transport of molybdate. However the mechanisms behind the adsorption of molybdate onto minerals in the subsurface at the Botlek are not entirely clear.
In PHREEQC, adsorption can be modelled as surface complexation reactions, with a surface complexation model. The next paragraphs will contain some background information about the surface complexation model used in this model.

2.10.1 Surface complexation models

A surface complexation model uses both:

1) The chemical bonding of solute species to surface atoms and

2) Electrostatic effects at the interface which are caused by the interplay of dissolved ions and the charged surface.

Due to the electric work related to adsorption, the adsorption equilibrium constant can be written as the product of the intrinsic constant (K_{intr}) and the coulomb term (K_{coul}):

$$K_{app} = K_{intr} \cdot e^{\left(\frac{-F \cdot \Delta Z \cdot \Psi_0}{R \cdot T}\right)} \tag{2.19}$$

PHREEQC has two surface complexation models. One is based on the work done by Dzombak and Morel (1990). They compiled data and developed a coherent set of intrinsic constants when using the diffuse double layer model (DDL). In this PHREEQC model, the diffuse double layer model is applied.

2.10.2 Diffuse double layer model

The diffuse double layer model has few adjustable parameters. The database in PHREEQC, specifically the minteq.v4 database, contains intrinsic constants for molybdate, making it useful for this research. Additionally, research done by Stollenwerk (1998) indicated the diffuse double layer model gave good results for modelling the surface complexation of molybdate.

2.10.3 Surface complexation reactions

The adsorption reaction between a hydrous oxide and a molybdate ion happens through the release of protons from surface hydroxyl groups (≡SOH) and the formation between molybdate and the remaining surface oxygen atom. These formulas can be found in the PHREEQC database minteq.v4, along with the intrinsic constants, and are used in the model:

$$\equiv SOH + MoO_4^{2-} + H^+ \rightarrow \equiv SMoO_4^- + H_2O \quad (2.20)$$

$$\log K_{intr} = 9.5 \quad \text{(strong)}$$

$$\equiv SOH + MoO_4^{2-} \rightarrow \equiv SOHMoO_4^{2-} \quad (2.21)$$

$$\log K_{intr} = 2.4 \quad \text{(strong)}$$

$$\equiv SOH + MoO_4^{2-} + H^+ \rightarrow \equiv SMoO_4^- + H_2O \quad (2.22)$$

$$\log K_{intr} = 9.5 \quad \text{(weak)}$$

$$\equiv SOH + MoO_4^{2-} \rightarrow \equiv SOHMoO_4^{2-} \quad (2.23)$$

$$\log K_{intr} = 2.4 \quad \text{(weak)}$$

There is not a lot of information in the literature concerning these equations. Stollenwerk (1998) used values for K_{intr} that are more or less the same. Therefore, the model contains the values as given in the PHREEQC database.
Because the extent of adsorption due to heterogeneities on the mineral surface can differ, the surface sites have been divided in weak and strong sites; the latter being the less abundant sites. The ratio between the amount of strong and weak sites is a parameter given in the model, which is then linked to the formulas above.
The intrinsic constants above are related to the adsorption equilibrium constant as seen in formula 2.19. K_{coul} can be written as an exponential term, in which the relationship with surface potential (and thus adsorption) becomes clear:

$$K_{app} = K_{intr} \cdot e^{\left(\frac{-F \cdot \Delta Z \cdot \Psi_0}{R \cdot T}\right)} \quad (2.24)$$

With ΔZ the change in the charge of the ion, F the Faraday's constant in Coulombs/mol, R the gas constant in 8.314 J/mol/K, T the absolute temperature in K, and Ψ_0 a the surface potential in V.

2.10.4 Surface charge and surface potential

The surface potential Ψ_0 arises when the surface charge exhibits a force on the ions in the adjacent solution. The surface potential can be related to the surface charge through the Gouy-Chapman theory:

$$\sigma = 0.1124 \cdot I^{\frac{1}{2}} \cdot sinh\left(\frac{-F \cdot \Delta Z \cdot \Psi_0}{2 \cdot R \cdot T}\right) \tag{2.25}$$

With σ as the surface charge density in Coulombs/m², I the ionic strength in mol/L and z the valence of a symmetrical background electrolyte.
Surface charge and ionic strength are calculated by PHREEQC, based on the values given for the parameters that the double diffuse layer model requires. With that, surface potential will be calculated which then gives the adsorption equilibrium constant and thus the degree of adsorption.
The amount of surface charge is based on the values given for the parameters in the model: surface site density and surface area. Values for these can be found in the literature. In the chapter methods, it will be described why the values for these parameters where chosen and how they were applied in the model.

2.11 Solubility

In PHREEQC, the solubility of the mineral on which the adsorbent adsorbs is expressed by the solubility product. The equilibrium between the ions in a solution and the mineral is given by this K. For example, the mineral goethite:

$$\text{a-FeOOH} + 3\ H^+ \rightarrow Fe^{3+} + 2\ H_20 \tag{2.26}$$

$$\frac{(Fe^{3+})}{(FeOOH)(H^+)^3} = K \tag{2.27}$$

The activities of the substances can be indicated with the ()-brackets. The equation can be rewritten for a given temperature. K is then constant and the activities of water and goethite are also constant and defined as 1. As a result, you can rewrite the equation:

$$(Fe^{3+})(H^+)^{-3} = K \tag{2.28}$$

Or, alternatively:

$$\log (Fe^{3+}) = \log K - 3\ pH \tag{2.29}$$

The solubility and precipitation of iron oxides determine how many surface sites you have available, which, as we saw, is an important parameter in the degree of adsorption.

3.

Methods

3.1 Setup

To model the geochemical behaviour of molybdenum in the subsurface at the Botlek, groundwater measurements from the field will be supplied as input for the geochemical modelling code PHREEQC. Earlier reports done by Bk Bodem (2012a, 2012b) and Deltares (2012) provide information about the site of the Botlek: the history of the site, basic introductions to the production processes, and the global situation of the contamination now and in historic perspective. For groundwater velocities and information about the geology, the 3D groundwater simulation program iMOD will be used. Measurement wells are located across the site, which provide samples at different depths. The actual situation about molybdenum in the subsurface is largely unknown, except from measurements taken from the wells. Information about the geochemical behaviour of molybdenum is also still unknown. The setup of the modelling part is to use PHREEQC to make a 1D model that can describe the behaviour of molybdenum with time and depth, given the provided groundwater measurements.
It is important to realise the modelling of the subsurface comes with uncertainties, especially in the case of molybdenum in the Botlek, where there is little information known beforehand. Initial concentrations are not known, nor the extent of the pollution. Only molybdenum concentrations from wells on the location are known, and these groundwater measurements can be done incorrectly and sampling errors can occur. Furthermore, it is very difficult to categorize geochemical processes as these occur less straightforward as often described in literature.
Throughout the modelling, assumptions have been made, to deal with these inaccuracies in groundwater measurements and uncertainties regarding the geochemistry of the subsurface at the Botlek. With a representative model, different scenarios can be constructed, adjusting specific parameters, and run with a different total simulated time. The aim of this study is to make a model that can make concentration-depth profiles from the start of the contamination in 1966, till the time of the last measurements, 2014, and make predictions about the future. Therefore, the setup is to model transport in such a way that graphs with results for 10 years, 20 years, 30 years, 40 years, 48 years, 100 years and 500 years can be plotted. The processes behind transport in the subsurface are already explained, as well as the implementation in PHREEQC. The next paragraphs contain a description of iMOD and PHREEQC, and the different functions of the latter that were used.

3.2 iMOD

Because a good understanding of the subsurface is needed, information about the geology and groundwater velocities will be extracted from MODFLOW. iMOD is a special graphical user interface and includes an accelerated version of MODFLOW, a program created by the United States Geological Survey (USGS). MODFLOW is a 3D finite-difference groundwater simulation model suitable for complex groundwater flow calculations and modelling. The GUI iMOD allows the user to zoom in or out on a particular area with the gridsize performing up- and down scaling to adjust to the resolution of the available data (Vermeulen, 2006); i.e. there is no need to construct a new grid for taking a closer look at a particular area.
For the particular information needed, basic functions of iMOD are used. Specific IDF files representing transmissivity values of the subsurface are loaded in iMOD, and based on characteristic values for transmissivity of geological layers, a simplified construction of the subsurface can be given.
Groundwater velocities in iMOD can be taken from particle flow paths. Specifically, one particle flow path has been taken for the area of Climax, giving flow velocities representing the different soil types.

These flow velocities can then be used for the transport component in PHREEQC.

3.3 PHREEQC

PHREEQC (version 3), or, pH-REdox-EQuilibrium, is a computer program capable of simulating chemical reactions and transport processes in natural or polluted water, in industrial processes and in laboratory experiments.
PHREEQC can be used for a variety of purposes. One of these is modelling the 1D transport, including diffusion and dispersion, and the subsequent interaction of the aqueous solution with minerals and adsorption surfaces. For a complete overview of the numerous possibilities of PHREEQC, the USGS contains a page dedicated to the program containing detailed information (Parkhurst and Appelo, 2015).
PHREEQC works with keywords and associated data blocks. The data blocks begin with a line containing the keyword, and on additional lines the data and information are stored. The keywords and the associated data are read from a database file that is defined at the beginning of a run, which contains the definitions for all the elements, exchange reactions, surface complexation reactions, mineral phases, gas components, and rate expressions. This data can then be adjusted in the input file by keyword data blocks.
First, the database is read, after which the input file is read until the first END keyword is encountered. The specified calculations are then performed. This process of reading data from the input file until an END followed by doing the calculations is repeated until the end of the input file. The calculations defined by keyword data blocks and completed with an END is a "simulation". A series of one or more simulations in the same input data file and calculated during the same invocation is called a "run". Below is a list of all the keyword data blocks that will be part of the model for the model.

3.3.1 Functions used

Database

The database is the keyword data block that links the used database to your model. PHREEQC has 9 databases that it can use, each containing definitions for all the elements, exchange reactions, surface complexation reactions, mineral phases, gas components, and rate expressions. These databases are compiled from numerous sources, and each database is suitable for a specific set of simulations. This model uses the wateq4f database. Not all information needed is in this database; hence it needs to be expanded. To realise this, specific chemical reactions have been taken from other databases and literature and have been added to the model.

Surface species

This keyword data block defines the reactions and equilibrium constants for the surface species used in the input file. This includes surface master species. This data block is often included in the database file used and only additions and modifications are included in the input file. However, the wateq4f database doesn't contain the proper reactions for the surface complexation of molybdate, so the proper reactions and equilibrium constants were taken from the minteq.v4 database and added to the model. The standard set of databases contains all sorts of surface species, defined by Dzombak and Morel (1990). The master surface species are Hfo_w and Hfo_s; these stand for the weak and strong binding sites on ferrihydrite.

Solution master species

This keyword data block defines the correspondence between element names and aqueous primary and secondary master species, with lines for each element. Furthermore, the lines contain the alkalinity contribution of the master species, the gram formula weight and the element gram formula weight. For

every major element and its primary and secondary master species, it is defined in the databases; however, the wateq4f database didn't contain molybdenum, so it was taken from the database minteq.v4 and added to the model. The model of this model contains added elements for Fe^{2+} and Fe^{3+} which have been split in Fe_di^{+2} and Fe_tri^{+3}, to account for kinetic modelling, which will be covered later.

Solution species

This keyword data block defines the chemical reactions, equilibrium constants, and activity-coefficients parameters for each aqueous species. Parameters that are used to calculate specific conductance, multicomponent diffusion, density, and enrichment in the diffuse layer of surfaces, can also be written here. This data block is included in all database files, but additions and modifications can be added in the model. The wateq4f database doesn't contain any information on the behaviour of molybdate, so it was taken from the minteq.v4 database and added to the model.
This data block in the model contains a lot of extra chemical reactions with the adjusted Fe^{+2} and Fe^{+3} elements, Fe_di^{+2} and Fe_tri^{+3}, which are all defined for kinetic modelling.

Phases

This keyword data block defines the name, chemical reactions, equilibrium constants, temperature dependence of the equilibrium constants for minerals used in the model that can be used for speciation, batch-reaction, transport or inverse-modelling calculations. Molar volumes can also be defined for solids. The majority of solids can be found in the database, however, the adjusted Fe_di^{2+} and Fe_tri^{3+} elements in the phases have to be dealt with, so this data block has been included in the model with the important, adjusted, phases in it.

Equilibrium phases

This keyword data block defines the amounts of a combination of pure phases that can react reversibly with the aqueous phase. The phases in this keyword data block come into contact with an aqueous solution and will either dissolve or precipitate to achieve equilibrium or will dissolve completely. The pure phases are minerals with fixed composition. The amount of the phase can be denoted, as well as the saturation level of the phase.

Surface

This keyword data block defines the properties of each surface in a surface assemblage: the amount and composition of the used surfaces is given. A surface assemblage can consist of multiple surfaces and each surface may have multiple binding sites, which are denoted by lowercase letters following an underscore. Different types of surface are available, and this model uses the diffuse-double layer surfaces (Dzombak and Morel, 1990).

Solution

This key word data block defines the composition and temperature of the initial aqueous solution that is modelled. It's the composition with which you run all calculations. The composition can be adjusted for individual element concentrations. All the concentrations given are converted internally to units of moles of elements and element valence states which includes hydrogen and oxygen. Speciation calculations are performed on all solutions that are defined by the SOLUTION data blocks, and each solution can then be used in further simulations; e.g. transport and batch-reaction. The aqueous solution needs to be divided into the measurements obtained from the field. The model has the aqueous solutions divided in multiple data blocks. SOLUTION 0 – m denotes the influent, which is in this case a measurement of its own. SOLUTION m – n denotes the composition of subsequent measurements. These SOLUTION data

blocks have been divided in amount of cells to account for the difference in flow velocities in the subsurface. The TRANSPORT data block will explain this more.

Use

This keyword data block is applied to allow a specific solution to be used for a simulation. In this model, it precedes the KINETICS and RATES data blocks.

Kinetics

This keyword data block is applied to specify kinetic reactions and parameters for batch-reaction and reactive-transport calculation used in the model.

Rates

Defines the mathematical rate expressions for the kinetic reactions defined in the KINETICS data block. The mathematical rate formula for the reduction of sulphate by organic matter is given in the wateq4f database of PHREEQC. The amount of organic matter and the total time for the rate law are important factors in determining the amount of sulphate that can be reduced.

Transport

Defines the simulation of one-dimensional (1D) transport of solutes and water in the model, due to processes of advection, dispersion and diffusion. Cell sizes, flow velocities, total runtime are all determined in this data block. Runtimes for the total model and flow velocities for different depths can all be adjusted. Chapter 2 contains a more detailed description for this data block.

Selected output

Data block that creates output suitable for processing in excel. All relevant parameters needed for conclusions are written in this data block.

3.4 Measurements from the Botlek

The production processes of Climax started in 1966, and it is presumed the contamination also started around this time. The measurements provided however, are taken in December 2014. Because the initial degree of contamination is not entirely clear, the most recent measurements are taken and used as the input for the modelling assignment. Ideally, over a time span of 48 years, you want to obtain the distribution as it would be now. If this distribution can be approached, predictions can be made about future concentrations.
Measurements of concentrations in the groundwater at the Botlek area are provided by 2 companies: UT2A and MWH Global. UT2A has only measured molybdenum, specifically molybdate, on the Climax area and the Lyondell area. Divided in 2 files, MWH Global has not only measured molybdenum, but a list of entire chemical constituents. These are taken from measurements wells only from the Climax area, as measurements from the Lyondell area are not yet provided.
Target values, intermediate values and intervention values have already been explained in chapter 2, with previous measurements of molybdenum. The MWH global measurements for my PHREEQC model are taken from the same measurement wells; divided in different areas. A position of a measurement well has multiple depths from which samples were taken. Considering PHREEQC is a 1D modeling program, it seems logical to take the location of one measurement well with multiple samples at this depth, so a clear pattern of chemical processes with depths can be chosen. Initially, this was the idea, however, not every measurement well has samples from every possible depth – seven – and therefore, the choice was made

to combine samples from different wells in a short range of each other. But even this proves difficult as it cannot be assumed that all samples taken completely represent the location where they are taken.
The MWH Global measurements contain pH and ORP values. The depth on which the well extracts its samples is also given, in centimetres below the reference sea level. Furthermore, a list of species of the aqueous solution is given, in either mg/L or µg/L. As molybdenum measurements are supplied in µg/L, this notation throughout the report for molybdenum values will be used. The ORP values (i.e. reduction potential) are not used in the model anywhere as they are often unreliable: they can give a rough indication of redox conditions, but correctly measuring this is a task very prone to errors.
The measurements provided seem to be contradicting as they suggest different redox conditions in the subsurface at the same depth. PHREEQC reads the composition and it will perform some adjustments on the solution making it stable (i.e. perform reductions and oxidations with consequences for your starting solution). For a groundwater solution that you can model with, it is necessary to make certain adjustments so that the solution is stable.

3.5 Groundwater quality

Looking at the measurements from the field, two things are distinct: the amount of molybdate in the subsurface is highest near the surface and it declines with depth. Sulphate appears to have the same pattern.
The measurements for ferrous iron in the subsurface appear more random. They have relatively high concentration in the sand layer and the clay layer, and less in the anthropogenic layer and the aquifer. There does not appear to be any sort of trend.
As proposed as a theory in chapter 2, the reduction of sulphate and formation of sulphides and the subsequent precipitation reaction with molybdate could be an explanation for the declining amount of sulphates. To test this hypothesis, these reactions have been added in the extended database (Allison et al., 1991; Stumm and Morgan, 1991), which makes it possible for these precipitates to form. The kinetic reduction of sulphate to bisulfide (HS^-), by organic matter, can be given by:

$$2\ CH_2O + SO_4^{2-} \rightarrow 2\ HCO_3^- + HS^- + H^+ \quad (3.1)$$

After which the equilibrium reaction between molybdate and bisulfide, forming molybdenite, takes place:

$$MoS_2 + 4\ H_2O \rightarrow MoO_4^{2-} + 6\ H^+ + 2\ HS^- + 2\ e^- \quad (3.2)$$

The electrons used from this reaction are donated by organic matter, which gets oxidized in the process.

$$0.25\ CH_2O + 0.25\ H_2O \rightarrow 0.25\ CO_2 + H^+ + e^- \quad (3.3)$$

To model the other possible explanation for a decline of molybdate, the reaction with ferrous iron, forming iron(II)molybdate, has also been added to the to the model:

$$FeMoO_4 \rightarrow MoO_4^{2-} + Fe^{2+} \quad (3.4)$$

There are however, some remarks to be made about the measurements. Some measurements have less total iron (ferric iron + ferrous iron) than ferrous iron. The measurements from the Botlek are not charge balanced: a solution needs to be balanced between positive and negative ions. This is not the case with these measurements as the charge balance is negative. Either concentrations of cations are incorrect, or certain cations are missing or not measured. Furthermore, the redox couples in many measurements are inconsistent as they suggest different redox conditions, the one being oxidizing and the other reducing. You would not expect nitrate to coexist with ammonia or methane as you would expect nitrate to be reduced to nitrogen, before the reduction of nitrite and carbon dioxide. Methane would only be present when other oxidizers are gone except for some sulphate. These are inconsistencies that cannot be

explained through the electron successor steps. However, complete redox equilibrium is seldom achieved in nature. Given enough time, the expected patterns of oxidized versus reduced species will tend to form. An alternative to waiting is to make some adjustments for these redox contradictions, which I intent to do.

3.6 Solutions in PHREEQC

The input for PHREEQC needs to be corrected for these redox contradictions. The measurements were all corrected in the same way: methane was removed from the system, as well as ammonium for the above mentioned reasons about redox contradictions. Nitrate was left out as well, essentially only keeping sulphate as the main reduced species. Throughout the literature, no evidence was found that suggests that molybdenum or molybdate reacts with methane, ammonium or nitrate, which allows it to leave these out without having important influence on the results.
Calcium cations (Ca^{2+}) and sodium cations (Na^{+}) were added to the solutions in the model and set to 'charge', to charge balance the solution. PHREEQC then calculates the amount of moles of calcium and sodium there needs to be in solution to correct for this missing balance. That amount of moles was converted to ppm, and subsequently used as input, ensuring the solution is actually charged balanced (or within an error margin of 1%). It is important to note that sodium can react with molybdate as indicated in chapter 2 (Xu et al., 2013). But this is not modelled as there is no sodium available in the solution, so the possibility of a precipitation reaction concerning sodium is not present.
The iron content of the solution was modelled as a sum of ferrous iron and ferric iron. However, the amount of iron in the solution is not stable as it is oxidized to goethite, and reducing nitrate in this process. Because this is undesirable, the amount of iron in the model was split in Fe_di and Fe_tri. This decoupling of ferrous iron and ferric iron is done because it disables the ability of ferric iron to be reduced to ferrous iron as that reaction is not included in the database. These 'new elements' Fe_di and Fe_tri have then been incorporated in reactions that originally included Fe^{2+} and Fe^{3+} and added to the extended database in the model.
To compare the models results with the actual situation, an initial approach to simplify the complexity of the geochemistry and the measurements was taken: all the measurements are averaged, over 5 different depths. The subsurface has been divided in a total of 5 redox zones – this makes it easier to distinguish between important depths, and model these depths as zones. The paragraph below gives a short description for these zones and what there redox conditions are. For PHREEQC, this is important as for the groundwater velocity, taken from MODFLOW, is used to flow along these redox zones and transport the contaminants further. When the particle flow path takes molybdate and sulfate along these redox zones, depending on the conditions, redox reactions occur which influence the state of molybdate or sulfate. The redox zones go from the top of the subsurface at 5 meters, to -25 meters, in the (deep) aquifer. The entire domain is thus 30 meters, which would be enough to model the downward transport of molybdate with time, into the aquifer.

3.6.1 Redox zones

Chapter 2, paragraph 4 described the theory behind redox conditions, providing us with context for the situation in the Botlek. With this information redox zones can be assigned that given insight in the geochemical situation in the subsurface and possibly be useful when modeling the subsurface in PHREEQC.
As the reduction of sulphate is of importance, and the decline of sulphate concentration with depth can clearly be seen from the measurements, the sulphate concentration was also modeled in the anthropogenic layer with the initial concentration set as such that with reduction, it would follow the same trend with depth as the sulphate concentrations from the measurements. To model this trend, the kinetic rate law has been adjusted until the result fitted the measurements. As the subsurface conditions

were described as all being ferric iron/sulphate reduction, in the model the subsurface was made in to one solution with different velocities, corresponding to the different redox zones. With the influent cell containing the molybdate and sulphate concentration, the subsurface itself only contains the other measured concentrations, and the added cations calcium and sodium to balance the solution.

3.6.2. Measurements used for parameterization molybdate and sulphate

The measurements of molybdate and sulphate where taken from measurements provided by MWH. These cannot yet be released; therefore a description of the choices regarding these values is given. MWH gave a table containing molybdenum, iron total and sulphate values for 3 places, the Northern site border, the Site center and the Southern site border. Divided over 7 depths, various measurements are given. For molybdate these averaged values were taken, for 5 depths:

Table 8: Molybdate measurements

Depth (m)	Hydrogeological unit	Concentration (µg/L)
+5	Anthropogenic sand layer	15000
0	Anthropogenic sand layer	235
-5	Sand layer	12
-11	Sand layer	1550
-20	Clay layer	30

Sulphate measurements were also given by MWH, for which also averaged values were taken:

Table 9: Sulphate measurements

Depth (m)	Hydrogeological unit	Concentration (mg/L)
+5	Anthropogenic sand layer	400
0	Anthropogenic sand layer	29
-5	Sand layer	<5
-11	Sand layer	102.5
-20	Clay layer	<5

3.6.3 Influent solution and column solution

As PHREEQC works with one influent solution, this needs to be the solution that contains the molybdenum input. Only one input was used for the model, which consists of the measurements taken in the anthropogenic layer. These have been averaged and then applied in the model, as a single solution. The measured concentration in the top layer was determined to be 15000 µg/L, so this concentration was taken as the influent (15 mg/L). The sulphate concentration was determined to be 400 mg/L. Solution 1 – 501 correspond to the initial conditions in the soil. These contain no molybdate or sulphate.

Table 10: Solution 0 – Influent

pH	6.86
Fe^{2+}	10.25 mg/l
HCO_3^-	260 mg/l
Cl^-	136 mg/l
SO_4^{2-}	400 mg/l
Ca^{2+}	30 mg/l
Na^+	200 mg/l
MoO_4^{2-}	15 mg/l

Table 11: Solution 1 - 501 – Column solution

pH	6.86
Fe^{2+}	10.25 mg/l
HCO_3^-	175 mg/l
Cl^-	50 mg/l
Ca^{2+}	40 mg/l
Na^+	50 mg/l

3.7 Adsorption

The adsorption of molybdate to goethite has been investigated and included in the model. Chapter 2 dealt with the theory behind adsorption, and how the parameters applied in PHREEQC influence the adsorption. As I apply the double diffuse layer model, I ran the model with different parameters given in the literature. Because the adsorption reactions in the PHREEQC database for molybdate are limited to the adsorption onto ferrihydrite, these were used. There are no measurements of the soil constituents, but goethite is a very common iron oxyhydroxide in the subsurface, and values for the parameters (surface area and surface site density) for goethite, which are used in the double diffuse layer, are well documented in literature. Therefore, adsorption was modelled on goethite instead of ferrihydrite. In the model, the surface sites of ferrihydrite have been coupled to the goethite in the subsurface. PHREEQC calculates the amount of surface sites and the subsequent adsorption on the available moles of goethite (which are given at the data block equilibrium surfaces). These values were taken from literature.
When using the double diffuse layer model in PHREEQC, you have 2 parameters to take into account: The surface site density (sites/nm^2) and the surface area (m^2/g). In the literature, the surface area is given in amounts per solid as well as the surface site density; and the values for parameters can differ. For the surface site density Mettler (2002) found a value of 2.9 sites/nm^2. The other value (1.97 sites/nm^2) applied in the PHREEQC model was taken from Goldberg (2013).
The standard for the specific surface area for goethite is, according to Van Der Laan (2008), between 20 and 200 m^2/g. Both the maximum and minimum value was taken. Because the study of the Botlek has no actual measurements, these values can give indications of the degree of adsorption according to literature. The surface area is given in amounts per solid as well as the surface site density. However, you want to have them per litre. Therefore, you will have to convert it so you can apply it in the model:

$$[\equiv SOH]_{tot} = \frac{A_S \cdot c \cdot 10^{18} \cdot N_S}{N_A} \tag{3.5}$$

With $[\equiv SOH]_{tot}$ as the total concentration of surface sites per volume solution, A_s the specific surface area in m^2/g, c the particle concentration in g/L, N_S the surface site density in sites/nm^2, N_A the Avogadro's number (6.0221413 * 10^{23} sites/mol). When the total concentration of surface sites per volume solution was calculated, it still needs to be converted to the amount of mol per mol goethite. This is done by calculating the amount of mol goethite present for every liter solution, after which the amount of surface sites per mol goethite is calculated. These values are then applied in the PHREEQC model. As mentioned, PHREEQC makes a distinction between weak and strong surface sites. As there are no measurements of this ratio, it is kept on 40 weak sites versus 1 strong sites, as this is the ratio used by Dzombak and Morel when they compiled the data for the adsorption with the double diffuse layer model. Four runs were done, with each the next parameters:

Table 12: Adsorption parameters

Scenario	Surface area (m^2/g)	Surface site density ($sites/nm^2$)	Strong surface sites (mol/mol goethite)	Weak surface sites
1	200	1.97	0.0582298	0.001455746
2	200	2.90	0.0066654	0.27
3	20	2.90	0.000145575	0.0058230
4	20	1.97	0.000036948	0.0014779

3.8 Solubility

In PHREEQC, precipitates are modeled using 2 parameters: initial amount of the substance (in moles/L) and the target saturation index, SI. The target saturation index of a mineral is defines as:

$$SI = log\left(\frac{IAP}{K}\right) \tag{3.6}$$

With IAP as the Ion Activity Product which stands for the activities in the water sample and K is the solubility product at equilibrium. The target saturation index indicates the propensity for a mineral to either precipitate, or dissolve to achieve equilibrium. If SI > 0, the solutions is supersaturated with the mineral and it will precipitate. If SI < 0, the solution is sub saturated with the mineral and the mineral will dissolve. If SI = 0, there is equilibrium between the mineral and the solution. If you put the SI in PHREEQC to 0, the mineral will either dissolve or precipitate to reach this desired equilibrium.
In the model, saturation indices are given after every shift of a solution into a higher cell, establishing new equilibriums, indicates which minerals would either dissolve or precipitate. These saturation indices are useful to gain insight in to what kind of precipitates would form with a given solution.

3.9 Transport

Transport was described in chapter 2, and table 13 depicts how transport was modelled in the model. Dispersion was set to 0 as it would not have meaningful effect on the results in this study. Diffusion has the default value of 0.3×10^{-9} m^2/s, although it is also not expected to have influence on the results. The total domain is 501 cells, divided in clusters of cells with the flow velocities obtained from MODFLOW.

Table 13: Transport parameters

Cells	501
Shifts	730
Time step	2074645
Flow direction	Forward
Boundary conditions	Flux flux
Lengths	50*0.1 110*0.045418145 145*0.041443124 181*0.049847514 15*0.334017966
Dispersivity	501*0
Punch cells	10
Punch frequency	152

3.10 Overview approach PHREEQC

The figure below illustrates the approach to the PHREEQC model:

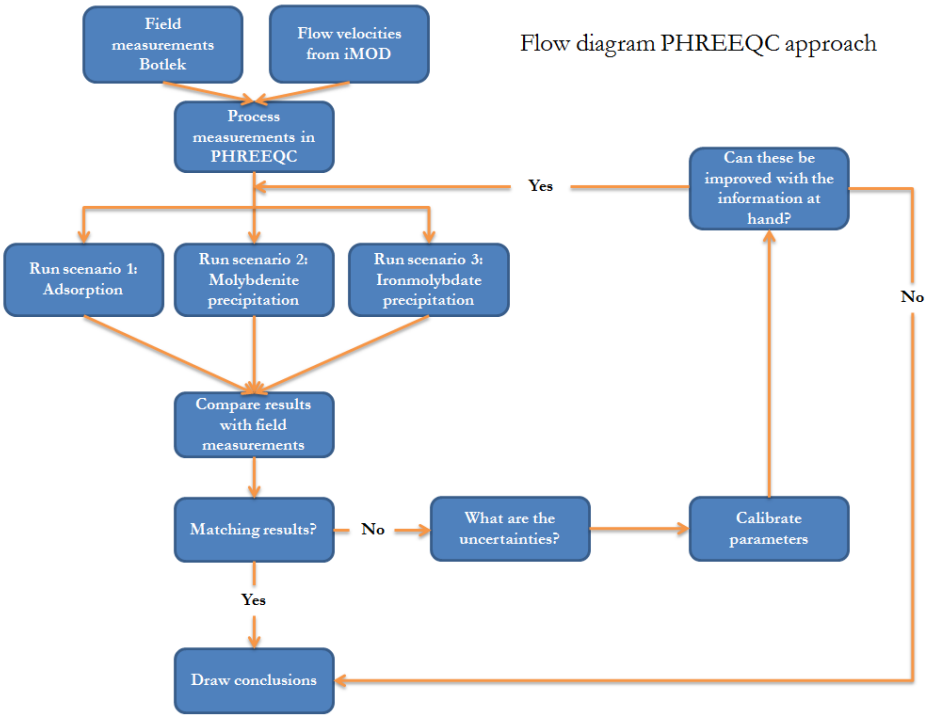

Figure 11: Flow diagram PHREEQC

4.

Results

All the results from the PHREEQC model have been plotted in graphs in which the x-axis depicts the concentration of the chemical constituent, and the y-axis depicts the distance of the subsurface. It runs from +5 meters to -25 meters, enough to cover all the measurements taken from the Botlek and to cover the distance to the aquifer. Because the large concentrations on the x-axis are often impractical to show on a small graph, the numbers were shortened, and therefore 'thousands' is given under the graph. The lines in the graph represent the years from which the results were plotted. It is assumed the contamination started in 1966, so T = 1966 represents the initial situation. The measurements provided are from 2014, so T = 2014 represents the end situation. The black diamond's show the actual measurements taken from the field in 2014.

4.1 Adsorption of molybdate

The range of the x-axis runs from 0 to 20000 µg/L and one graph shows the concentration of molybdate and the other graph shows adsorbed molybdate. In the scenarios with adsorption, no precipitation reactions have been modelled.

4.1.1 Adsorption scenario 1

Surface site area: 200 m^2/g
Surface site density: 1.97 sites/nm^2

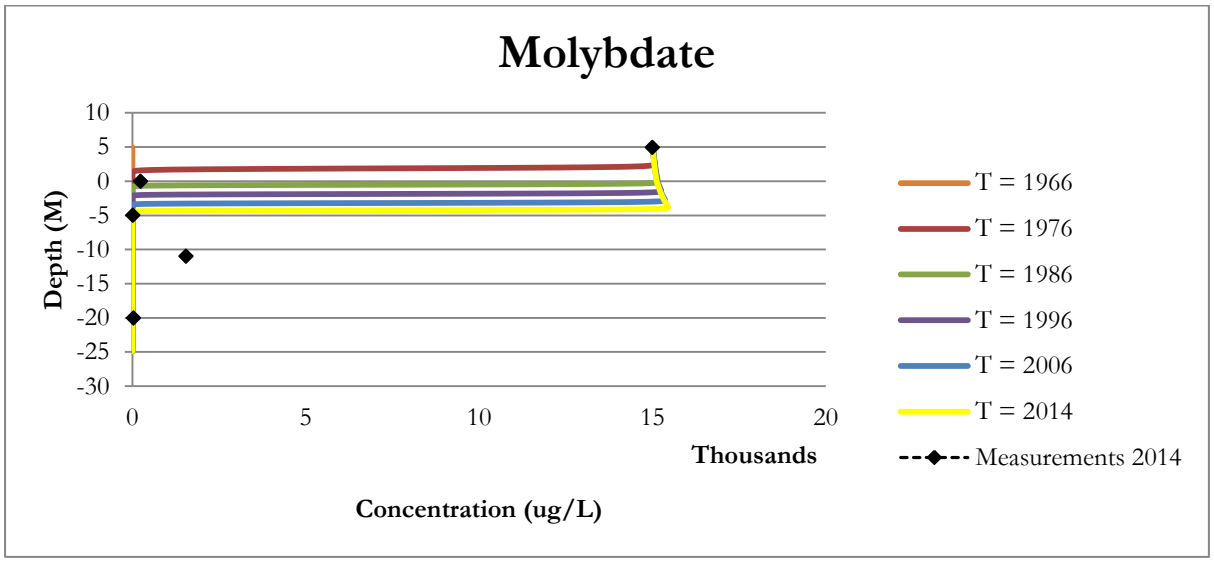

Figure 12: Concentration molybdate with depth, adsorption scenario 1

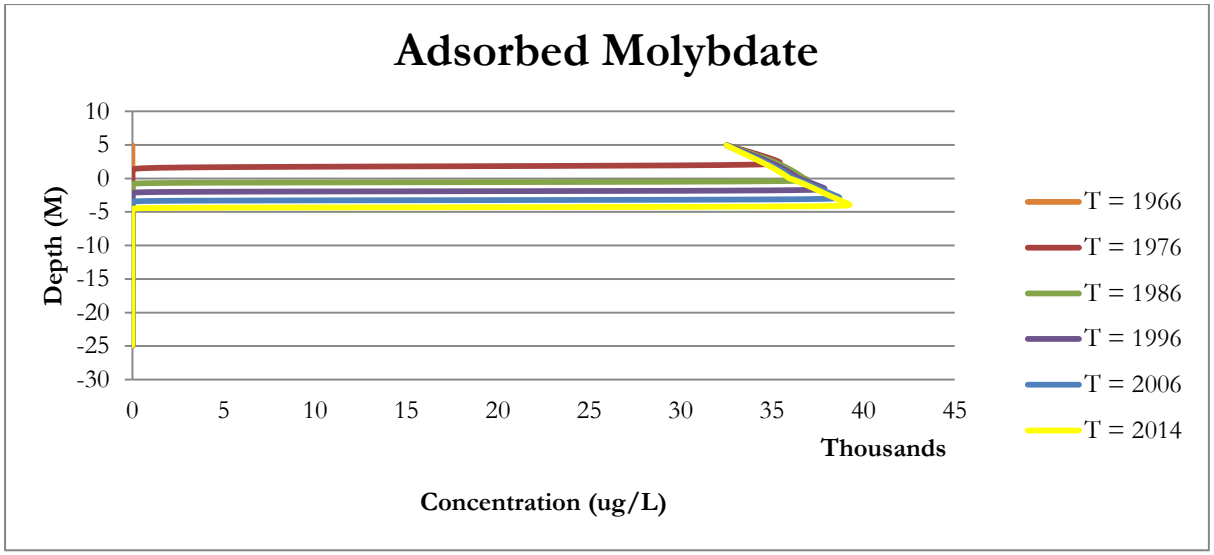

Figure 13: Concentration adsorbed molybdate with depth, adsorption scenario 1

In this scenario, with parameters from Van Der Laan (2008) and Goldberg (2013), the molybdate front shows a clear progression downwards with time. At T = 1966, there is no molybdate yet in the solution, but looking at the line representing T = 1976, molybdate has a value of 15000 ug/L, the initial influx value, which it stays for a couple of meters before it rapidly declines to 0, after which it stays zero. This trend is the same with the other years plotted: the concentration start from 15000 ug/L, slightly increases, and then declines to 0. The ultimate depth the molybdate contamination reaches is around -4 meters.
The adsorbed molybdate lines show a slightly different trend: after ten years (T = 1976), adsorbed molybdate has increased to around 35000 µg/L. The decline of the lines occurs at the same depth as where the decline of molybdate in solution occurs: both fronts are of course, linked to each other. With time, the amount of adsorbed molybdate increases with depth, as can be seen from the plotted lines from the later years. This can be explained by the increase of molybdate in the system with time. Eventually, in 2014, the amount will be almost 40000 ug/L, which is almost a factor 2.5 larger than the amount initially measured in the anthropogenic layer, which was the highest amount measured in the entire subsurface. Both the amount of molybdate and adsorbed molybdate never go deeper than -5 meters covering less than 10 meters in total.
This high amount of adsorbed molybdate seems very unlikely: more molybdate would be adsorbed than is measured in the subsurface. These parameters overestimate the amount of sorption significantly.

4.1.2 Adsorption scenario 2

Surface site area: 200 m^2/g
Surface site density: 2.90 sites/nm^2

Below, in figure 14 and 15, the results of adsorption in the second scenario are given. The surface site density was taken from Mettler (2002).
Based on theory, you would expect the second scenario to have the most adsorption of all scenarios: both surface area and the surface site density are largest values of all scenarios. The results suggest the same:

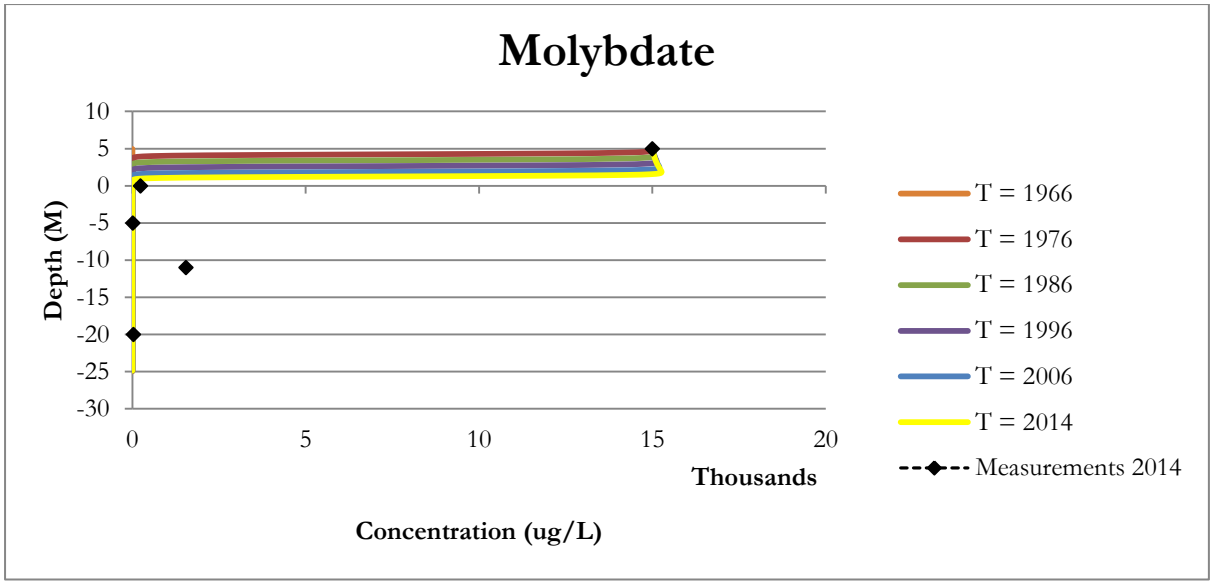

Figure 14: Concentration molybdate with depth, adsorption scenario 2

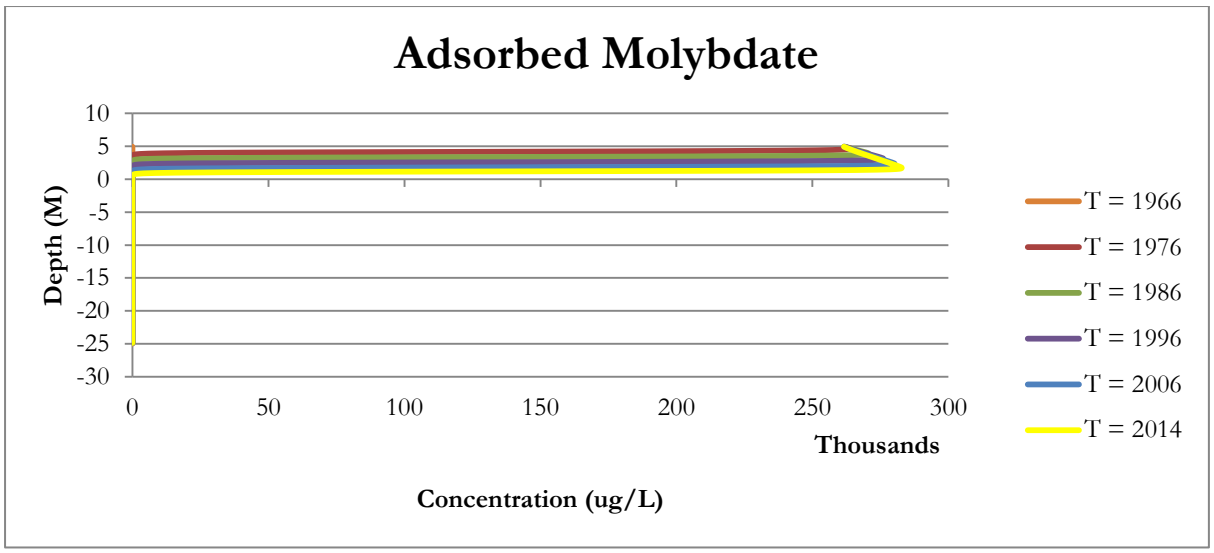

Figure 15: Concentration adsorbed molybdate with depth, adsorption scenario 2

The same trend as in scenario 1 can be seen: molybdate, starting with concentration of 15000 µg/L, initially travels a very short distance, and then rapidly declines to zero, while at the same time, the amount of adsorbed molybdate increases a bit, and then rapidly declines to zero as well, indicating the front of the molybdate contamination. However, the transport of molybdate in this scenario is less than in the previous scenario: both molybdate and adsorbed molybdate do not travel past the anthropogenic layer in the 48 years modelled, with these parameters of adsorption. The amounts of adsorbed molybdate are almost a factor 20 larger than the amount of molybdate in solution. This is a lot more than the amount of adsorbed molybdate in scenario 1.

Molybdate adsorption is highly overestimated with these parameters, as without any other process occurring in the subsurface that influences the fate of molybdate, you would expect the molybdate to travel further in 48 years, past the first 5 meters, which is not the case in this scenario. Furthermore, in this scenario, you would expect more molybdate measurements in the top layer with a very high concentration.

4.1.3 Adsorption scenario 3

Surface site area: 20 m^2/g
Surface site density: 2.90 sites/nm^2

Scenario 3 has, contrary to scenario 1 and 2, a very low surface site area (Van der Laan, 2008). Figure 16 and 17 below show the results of adsorption in the third scenario.

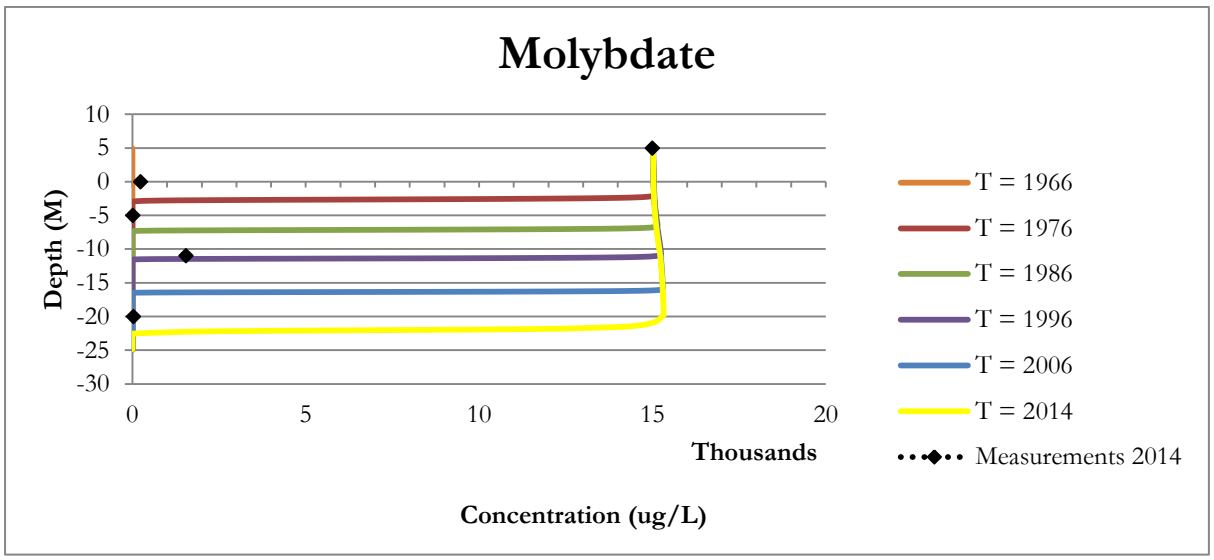

Figure 16: Concentration molybdate with depth, adsorption scenario 3

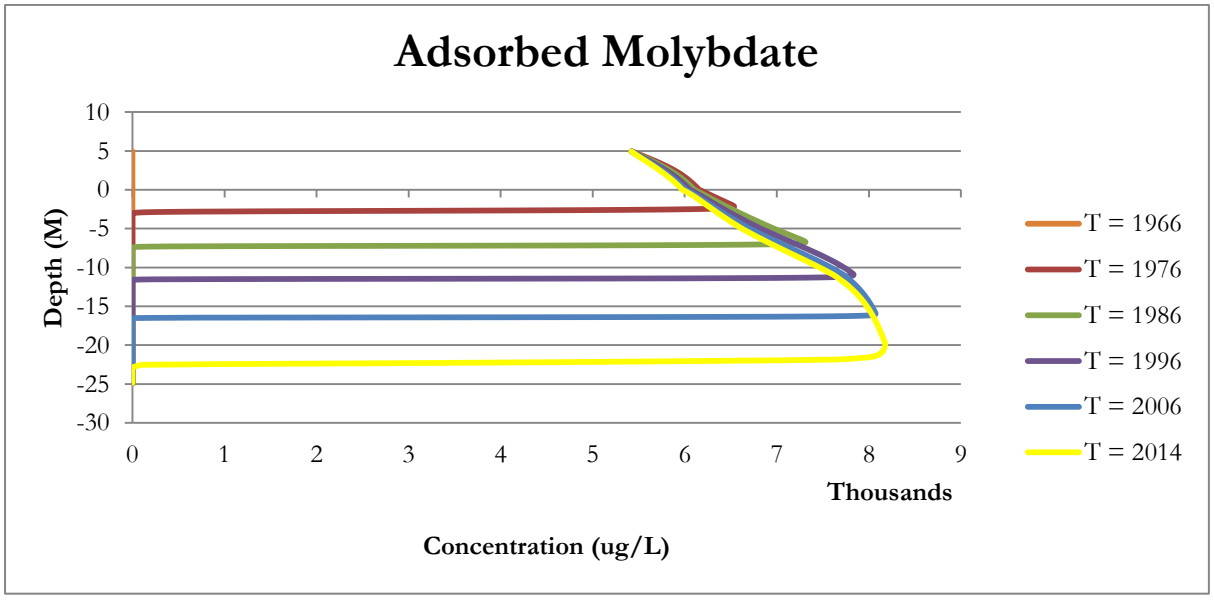

Figure 17: Concentration adsorbed molybdate with depth, adsorption scenario 3

There is now less surface area to adsorb on and you would expect less adsorption. The amounts of adsorbed molybdate are around a factor 2 smaller than the amount of molybdate in solution. The years plotted all show that molybdate travels deeper in the subsurface than with scenario 1 and 2, and reaches a concentration of 0 also later than in the earlier scenarios. The trend of molybdate concentration we saw in the previous scenarios, also applies here: apart from a slight increase in concentration, nothing is happening with the concentration with depth.
Adsorbed molybdate also follows the trend we saw earlier: it increases with depth, due to the extra input

of molybdate in the system. The amount however, is lower than in earlier scenarios, and both molybdate and adsorbed molybdate travel deeper, indicating a more realistic scenario given the measurements.

4.1.4 Adsorption scenario 4

Surface site area: 20 m^2/g
Surface site density: 1.97 sites/nm^2

Scenario 4 has, in addition to a low surface site area, a low surface site density (Goldberg, 2013). Figure 18 and 19 below show the results of adsorption in the fourth scenario.

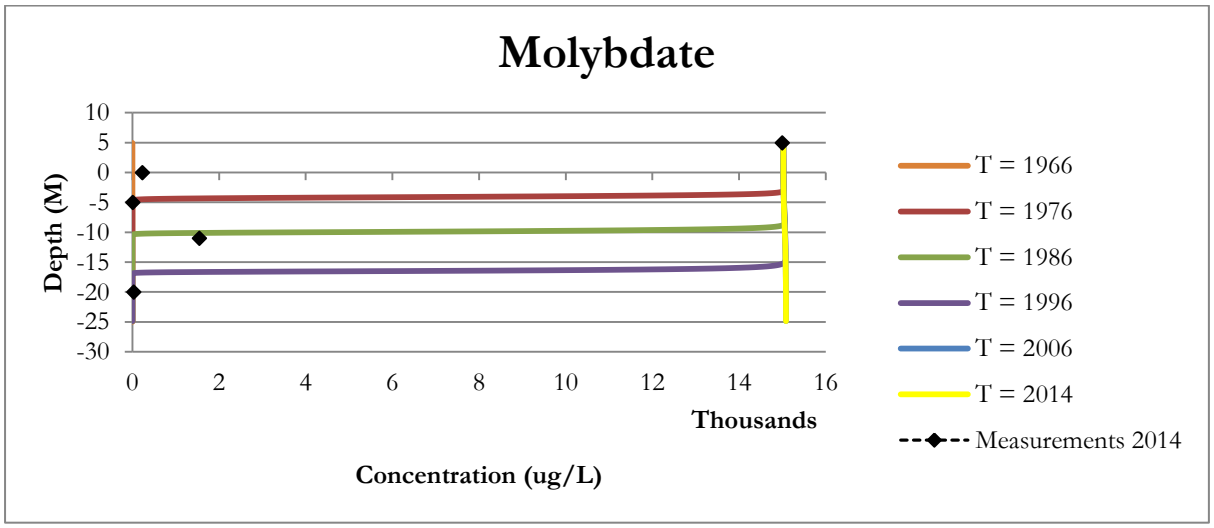

Figure 18: Concentration molybdate with depth, adsorption scenario 4

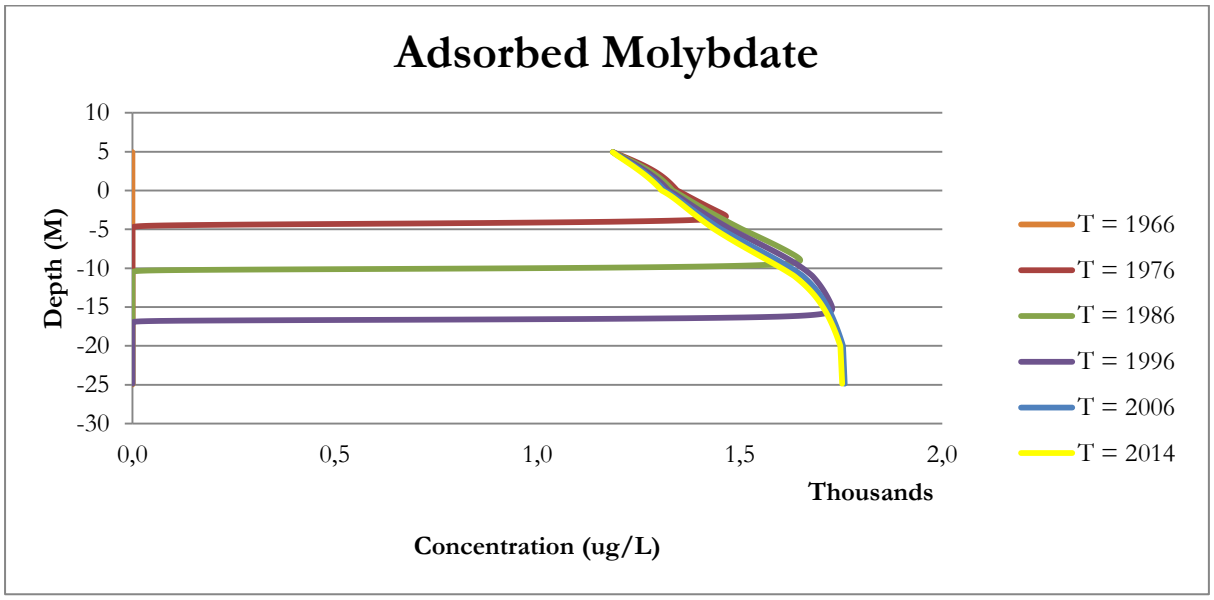

Figure 19: Concentration adsorbed molybdate with depth, adsorption scenario 4

Scenario 4 has the same surface area but less specific surface sites than scenario 3. There is now less surface area to adsorb on and you would expect less adsorption. The result emphasizes this: the amounts of adsorbed molybdate are now a factor 10 smaller than the amount of molybdate in solution.
When looking at the depth molybdate travels, according to the results in 2014, molybdate would be present in the aquifer in the same amounts as the initial input which is 15000 µg/L. Adsorbed molybdate

amounts are relatively low, but slightly increase with depth; the same pattern we saw in the earlier 3 scenarios. With these parameters, the degree of adsorption is too low to explain the behaviour of molybdate with depth. Specifically, the decline with depth cannot be explained with adsorption only.

The influence of the different flow velocities on the degree of adsorption is minimal. The curves from different years of each graph show the same pattern, regardless of the depths and velocity.
The results do not follow the 'general trend' of the measurements given by MWH, and the adsorption curves show the trend that the front of the contamination spreads downwards, but no change of concentration of molybdate can be seen: in scenario 4, the molybdate concentration in solution remains 15000 μg/L, in the other 3 scenarios, the concentration even slightly increases. Therefore, adsorption alone cannot explain the decrease of the concentration of molybdate in the subsurface of the Botlek. The parameters chosen in the first 2 scenarios also seem to overestimate adsorption, whereas scenario 3 and scenario 4 seem more realistic.
Initially, the idea was to model future scenarios, T = 100 and T = 500. The progress of the concentration fronts with time appears to be rather predictable and making time scenarios seems to be not really useful at this stage of the research of molybdate behaviour in the Botlek

4.2 Precipitation of molybdenite

In this run, the goal was to look at the precipitation of molybdenite. The formation of molybdenite requires the presence of sulphides. However, with ferrous iron and sulphides in solution, the formation of pyrite and mackinawite (FeS) is possible, therefore these reactions have been added in the model. There is no adsorption of molybdate.
The formation of sulphides occurs through the reduction of sulphate. This sulphate is introduced to the subsurface in the same way as molybdate, i.e. it is not present initially in the subsurface.
The results were plotted in the 6 graphs below.
First, looking at graphs 20 and 21, the relationship between the decrease of sulphate and the increase of sulphides can be seen. The decrease of the sulphate concentration with depth follows roughly the same trend as the measurements from the field. The measurement at a depth of -11 meters could be the result of a sampling error. This graph also shows the influence of the different flow velocities: at 0, a bend in the curves can be seen.
Figure 22 shows the pattern of molybdate concentration. It is the same for all the plotted times: molybdate slightly increases after which it very rapidly declines to 0. This all happens in the anthropogenic layer. The increase is due to the extra input of molybdate. In the first few meters, molybdate does not react with sulphides: the formation of pyrite seems more favourable as graphs 23 and 24 indicate that sulphides prefer to react and precipitate with ferrous iron. This suggests pyrite is thermodynamically more stable than molybdenite.
The decrease of molybdate happens at the same time molybdenite starts to form. The generated sulphides will react with available molybdate and instantly form molybdenite. The amount of molybdenite in the anthropogenic layer accumulates with increasing time, up to a concentration of 740000 μg/L. This can be seen in graph 23. Because of the precipitation of pyrite, it is lost from the solution, and accumulates in the anthropogenic layer. As soon as there is no more sulphate in concentration, the amount of ferrous iron in concentration increases – there are no more sulphides to react with.
At the same time, graph 21 shows the formation – increase – of sulphide concentration with depth. The increase doesn't start at the top of the anthropogenic layer: the first sulphides are immediately reacted with ferrous iron. Only after initially all the ferrous iron and then molybdate available has reacted, sulphides enter the solution. The front of the sulphide concentration can also be seen, being transported deeper in the subsurface. The decline of sulphides occurs when there is no more sulphate in solution.
The decrease of molybdate is the same for every year plotted, and suggests molybdate is not anymore

present at depths greater than +2. A molybdate measurement at a depth of -11 meters shows the same outlier that can be seen at the sulphate measurements: this too, is the result of a sampling error.

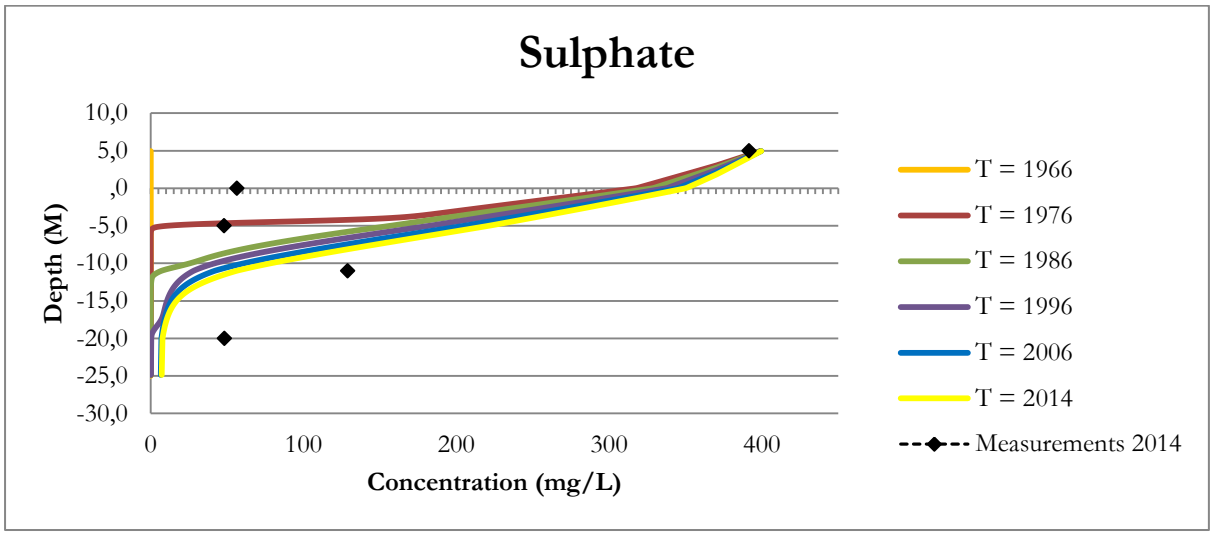

Figure 20: Sulphate concentration with depth

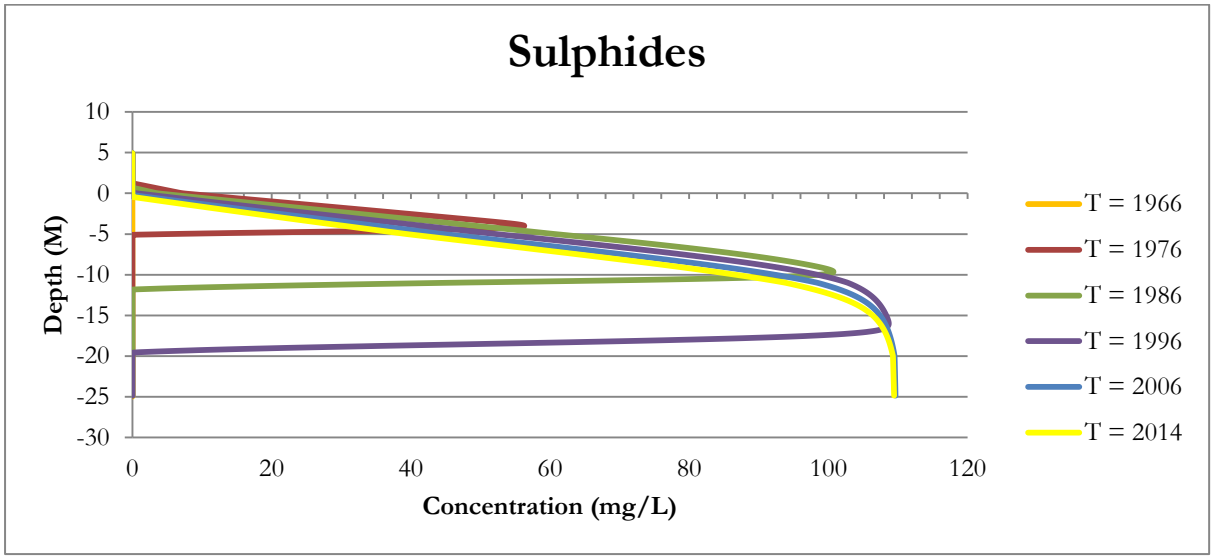

Figure 21: Sulphide concentration with depth

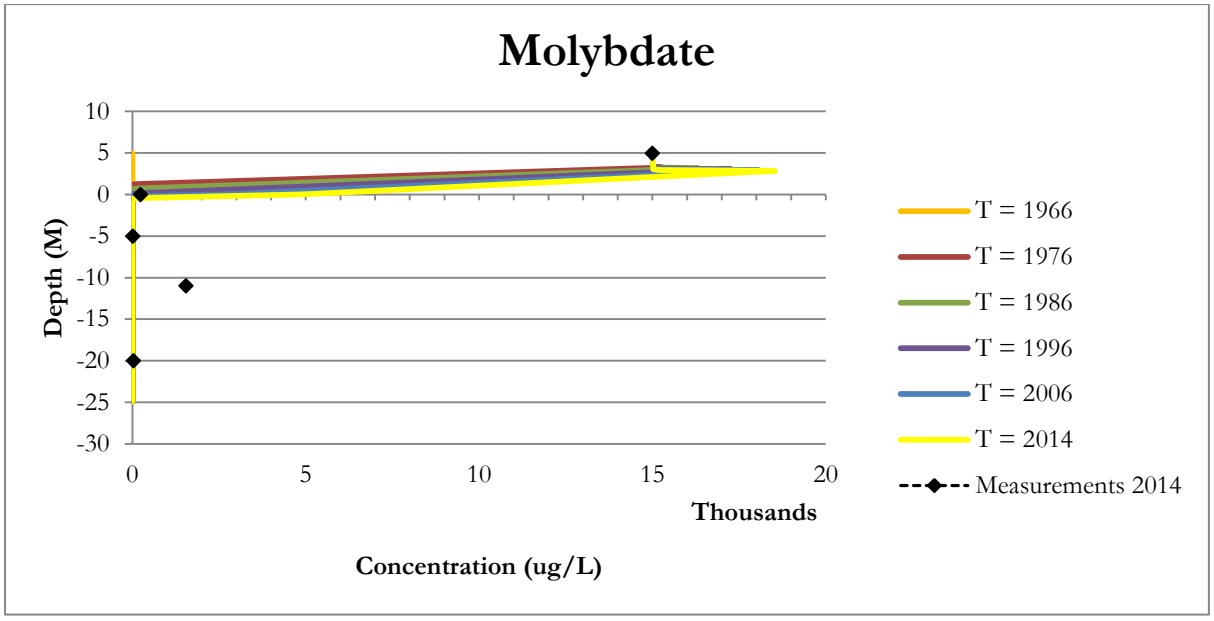

Figure 22: Molybdate concentration with depth

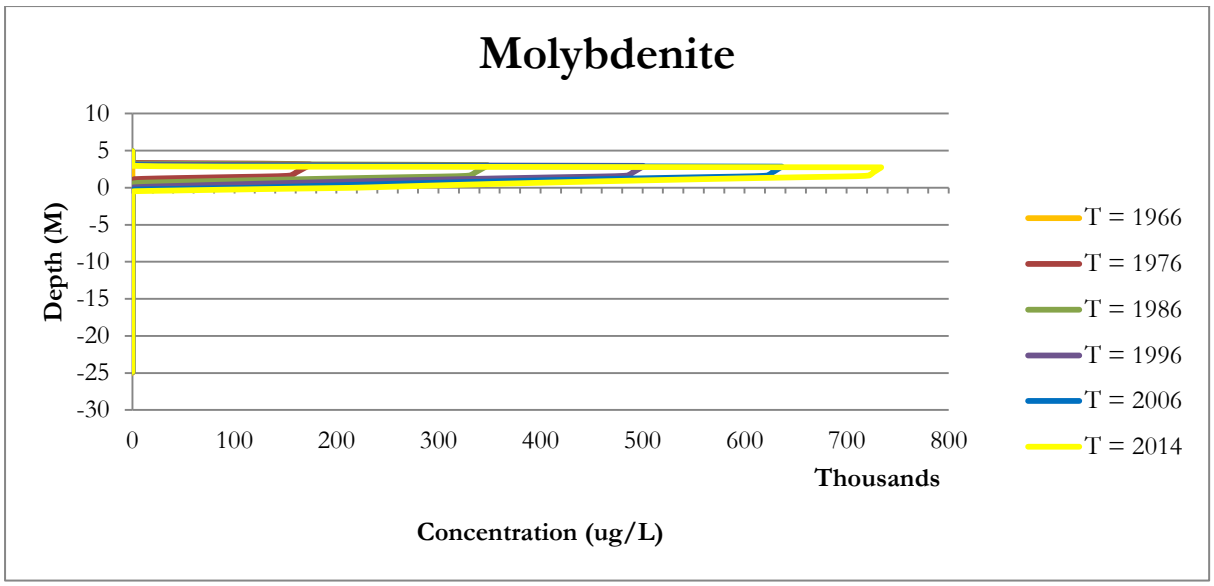

Figure 23: Molybdenite concentration with depth

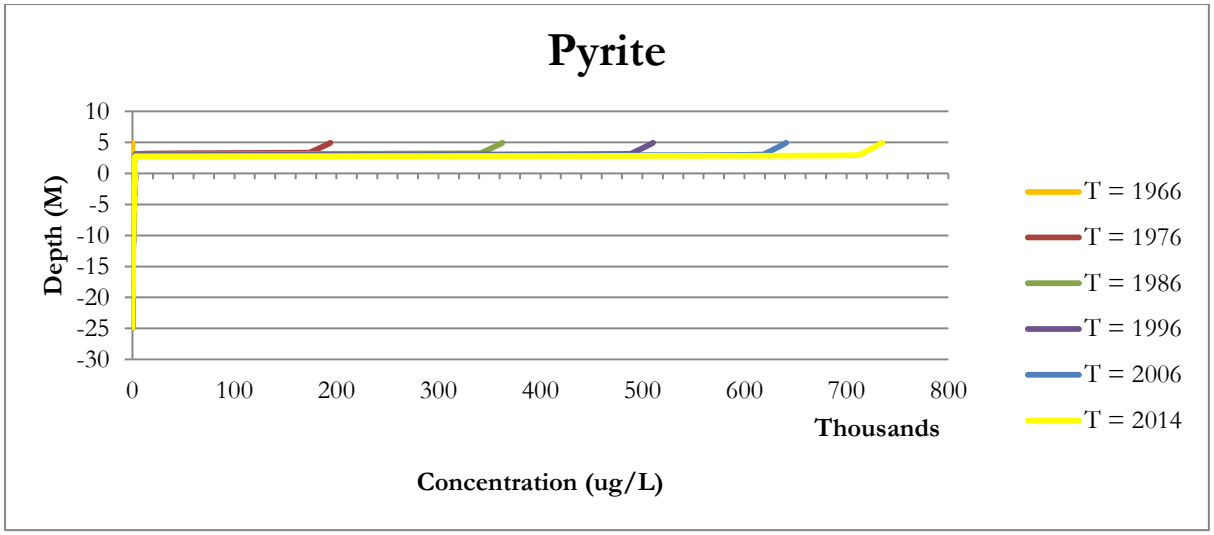

Figure 24: Pyrite concentration with depth

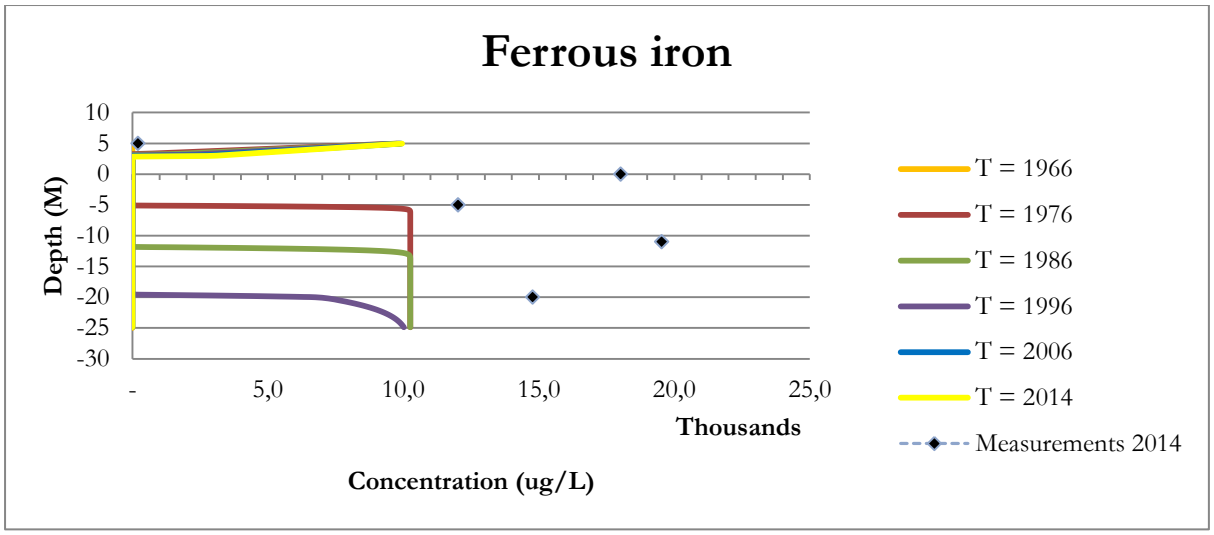

Figure 24: Ferrous iron concentration with depth

Without the formation of pyrite, all the sulphides would have reacted with molybdate and precipitated as molybdenite: the precipitation of pyrite can be seen as a limiting factor.
As mentioned, the results indicate that ferrous iron competes with molybdate for the available sulphides, and the results indicate that pyrite in this system would be found as well as molybdenite. Both concentrations show values of around 720000 µg/L. Also, pyrite seems to be formed earlier than molybdenite. However, this does not necessarily mean that in reality, pyrite would always form earlier than molybdenite. But it is beyond the scope of this research to make statements about the ratio in which these precipitates would be found in the field, and what would exactly be the dominant precipitation reaction occurring. There was no formation of mackinawite in this scenario.

4.3 Precipitation of iron(II)molybdate

In this run the precipitation reaction between molybdate and ferrous iron was modelled. There is no adsorption of molybdate. The other reactions that could occur are the formation of pyrite and mackinawite, both precipitation reactions between iron(II) and sulphides. Figures 26, 27, 28 and 29 below show the results.
Figure 26 shows the concentration of molybdate with depth. Like the other scenario's, the influx of

molybdate is 15000 µg/L. However, this initial concentration is not achieved in the solution: all the lines start at a concentration of ~1600 µg/L. The progression of the contamination front can clearly be seen. T = 2014 does not coincide with the measurements from 2014.
If we look at the figure 27 for iron(II)molybdate, all lines are exactly the same, with the line representing T = 2014 being visible.
Figure 26 and 27 show the concentrations of iron(II)molybdate and pyrite respectively, with depth. Although both sulphides and molybdate compete for ferrous iron, concentrations of iron(II)molybdate are 32 times larger than concentrations of pyrite. Clearly, the precipitation reaction between ferrous iron and molybdate is favoured. Both reactions, however, appear to happen instantaneously: the concentration decreases rapidly from the first meter, and the concentration does not advance with depth.
Figure 28 below depicts the graph for ferrous iron, which shows the measurements from 2014. The available ferrous iron in solution is lowered until there is no molybdate left to react with, after which it increases to 10 µg/L, and stays on this concentration.

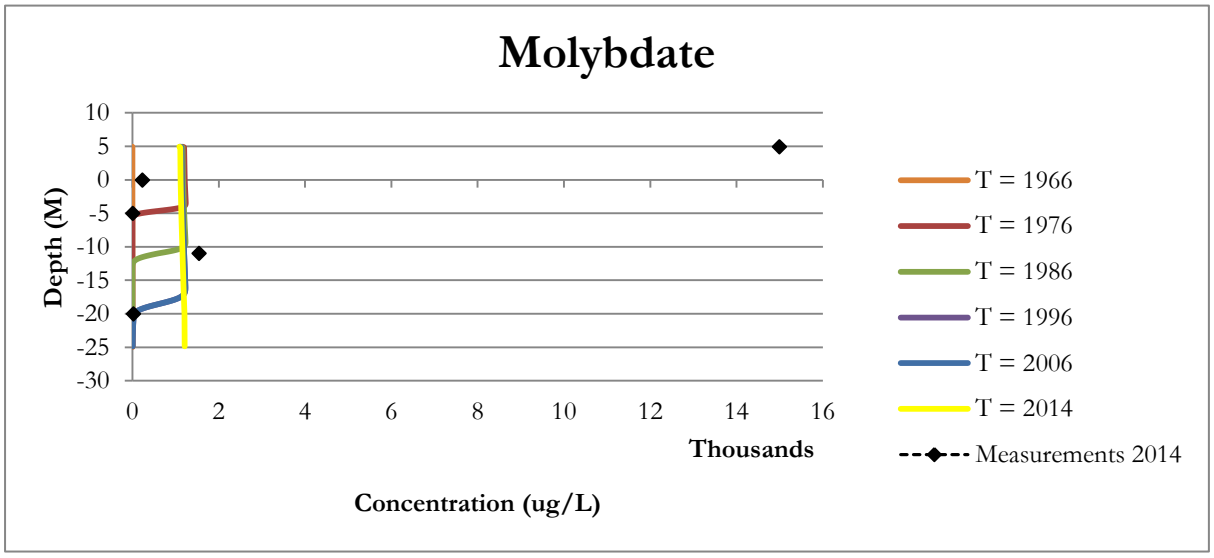

Figure 26: Molybdate concentration with depth

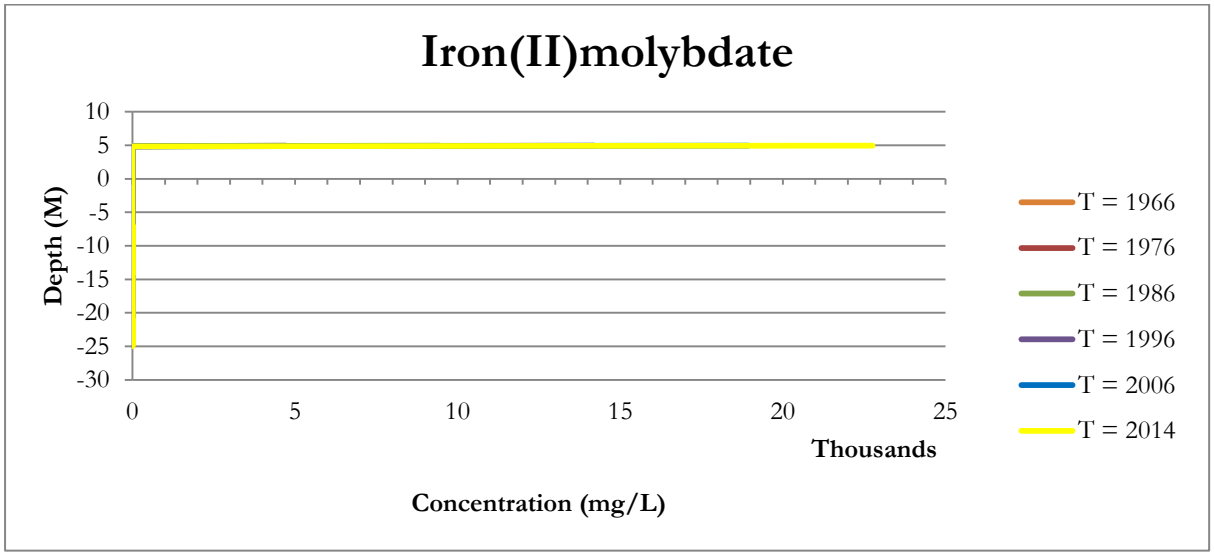

Figure 27: Iron(II)molybdate concentration with depth

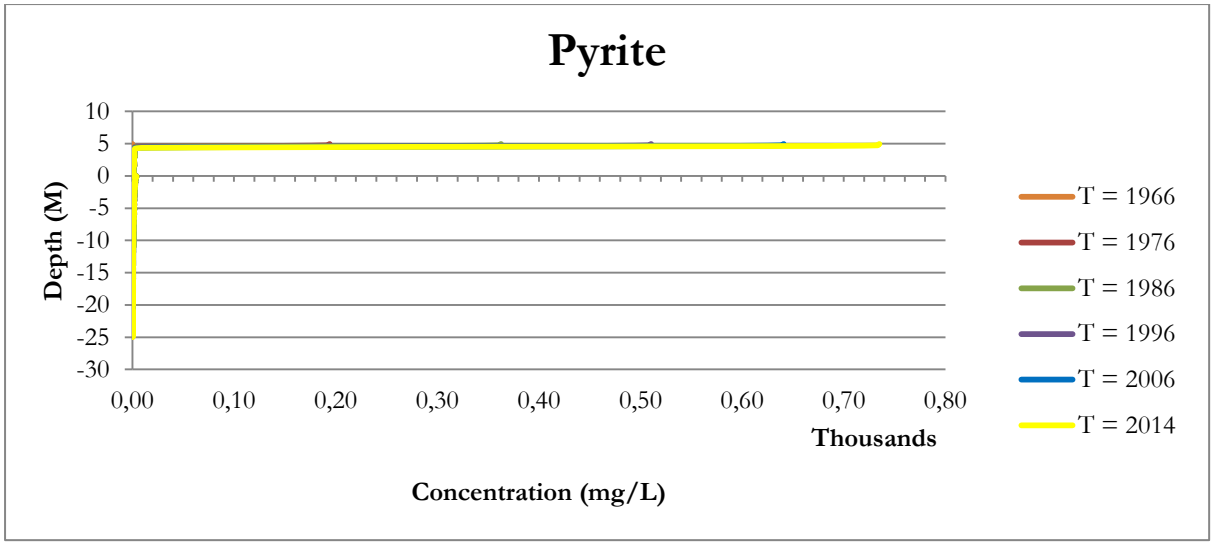

Figure 28: Pyrite concentration with depth

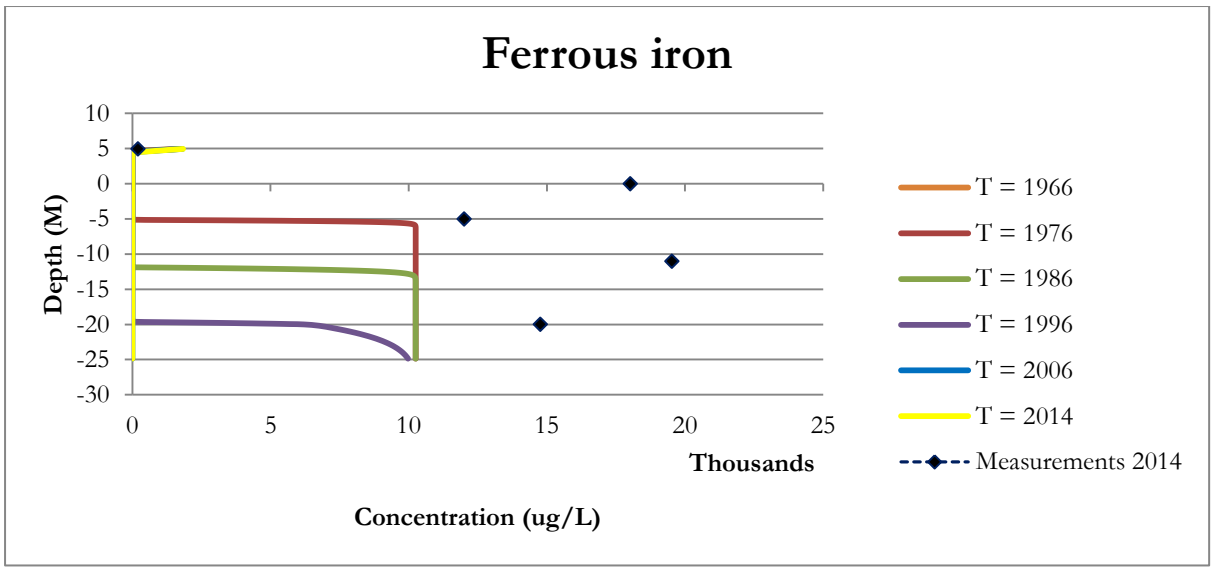

Figure 29: Ferrous iron concentration with depth

In this scenario, iron(II)molybdate is clearly the favourable reaction between ferrous iron and molybdate and ferrous iron and sulphides. Mackinawite was not formed in this scenario.

The precipitation reactions occurring in this scenario and the previous scenario between molybdate and sulphides clearly occur. However, much more cannot be said at this stage of the research. More explanation about this will be given in the conclusion and the discussion. Furthermore, these results clearly limit the possibility of future scenario and thus predictions: because nothing can be said about the time dependency of these reactions, running future scenarios with T = 100 and T = 500 is not useful.

5.

Conclusion and discussion

The purpose of this research was to investigate the geochemical behaviour of molybdenum in the subsurface at the Botlek. Based on measurements, it is known that molybdenum percolates through the subsurface, through the clay layer into the aquifer. However, what chemical reactions molybdenum undergoes in the subsurface is not clear. Earlier research indicates that molybdenum is possibly adsorbed in the subsurface, as the anion molybdate.
With the geochemical modelling program PHREEQC, an insight into the reactions and speciation of molybdenum can be given. Specifically, the precipitation reactions it can form, and the degree of adsorption that takes place. Furthermore the goal of this research was to gain more knowledge, about the time it will take to travel through the subsurface into the aquifer and to predict future scenarios.
After building a PHREEQC model with the given measurements from the field and information about molybdenum from literature, the following conclusions can be drawn:

1) The major reaction that will occur in the subsurface at the Botlek is between molybdate and sulphides. Due to the reducing circumstances in the subsurface of the Botlek, available sulphate will be reduced to sulphides, which react with molybdate to form molybdenite. Molybdenite will precipitate and be lost to the aqueous solution. The formation of pyrite, between ferrous iron and sulphides, will also occur in these circumstances and will compete with molybdate for sulphides.

2) Molybdate will also react with ferrous iron present, and precipitate as iron molybdate. In addition to this reaction, sulphides present can also react with ferrous iron and precipitate as pyrite, albeit in much lower concentrations.

3) Adsorption of molybdate onto goethite in the subsurface is occurring. The degree of adsorption is determined by the parameters for surface complexation models, which are taken from literature. Based on the results for adsorption, the conclusion can be made that more needs to occur with molybdate in the subsurface to explain the trend of the measurements.

This study shows that molybdate and sulphides forming molybdenite and the subsequent precipitation of this mineral is the most dominant reaction concerning molybdate, occurring in the subsurface of the Botlek. This determines the fate of molybdate. Sulphate, which infiltrates the subsurface, is reduced in the circumstances of the Botlek, forming sulphides, which in turn react with molybdate, forming molybdenite precipitation. This molybdenite will precipitate in the top layer, accumulate, and is thus lost to the solution in the subsurface. It is not clear how fast the precipitation reaction will occur. A competing factor in this process is the precipitation reaction between ferrous iron and sulphides, forming pyrite. However, with the information now, it cannot be said what precipitation reaction would be favourable as information regarding this was not investigated during this study.
When a mineral is supersaturated, as is the case with molybdenite in the Botlek, it can precipitate directly, but often, this is not the case. The degree of precipitation is dependent on time. To model this, it is essential to have information on the rate law of molybdenite precipitation and model it kinetically. This information on molybdenite is not available in literature and unfortunately the approach taken in this study does not give any information on the rate law of the reaction. Therefore more detailed information on the rate law of this reaction remains unknown.
Without this information, the reaction between molybdate and sulphides cannot be modelled correctly, taking the time it takes to form precipitates into account. Making future scenarios is therefore not useful either.

The same holds for the reaction between ferrous iron and molybdate. Molybdate enters the subsurface where it reacts with the available ferrous iron, forming iron(II)molybdate. In the results, this happens instantaneously. This cannot be modelled kinetically, as information about the rate law is missing. Therefore, predictions about the contamination with time cannot be made.
Molybdenum is an exotic element and is rarely found in the subsurface. Therefore, little research is done on its behaviour in the subsurface. Literature review provides little information on molybdenum/molybdate and its geochemical behaviour, and comparable studies are not at hand: industrial contamination studies are often well documented but not for molybdate.
Even the databases used in PHREEQC are not all equipped with the correct chemical data on molybdate. The available data from the field, the groundwater samples taken from measurement wells, provide the information needed for making a model to give insight into the situation.
This study provides a basis for further, more detailed research into the rate law of this reaction, such that more insights can be gained in the time dependency of this reaction and to predict precipitation rates.
The circumstances in the Botlek for adsorption of molybdate, pH and available sorbents, provide an environment in which adsorption plays a role, as was seen from the results, and it notably retards the transport of molybdate. It will however, only retard, and not prevent the downward transport of the contamination.
Based on the information at hand and the current state of knowledge of molybdenum and molybdate, these are the processes that are occurring in the subsurface. This study has not excluded possible scenarios and there is no evidence, based on the measurements used, that other factors or (chemical) processes are determining the fate of molybdenum.

5.1 Field measurements

Measurements taken from the field come with measure inaccuracies. This was already described in chapter 2. A model will be made based on the measurements that are available, even if these are not completely accurate. In the PHREEQC model, adjustments have been made to obtain solutions that can be modelled with. Extra elements had to be added to balance the solutions, and certain species had to be removed that were not useful for the model. Rough estimations of redox conditions were made and a similar approach to the conditions in the subsurface was done.
The measurements were not all from exactly the same set of coordinates, which could indicate some concentrations represent different subsurface conditions, or a different particle flow. These notions have been smoothed in taking average values in the PHREEQC run file. However, I'm of the opinion that this should not influence the results in a distinct way.

5.2 Adsorption

The results for adsorption on goethite give a clear pattern. In the review chapter 2, it is mentioned phosphate would compete with molybdate for available adsorption sites. However, the measurements from the Botlek contain no phosphate. Furthermore, the site at the Botlek has no recent history of agricultural activities, ruling out the possibility that elevated concentrations of phosphate could accumulate in the subsurface.
In the model itself, no distinction was made in the layers as they were given by MODFLOW. For the flow velocities, the velocities have been adjusted for the different layers and applied in PHREEQC. The literature clearly made distinction between different soil types and their relation with adsorption. These distinctions could make a difference in the degree of adsorption, but it was chosen not to apply this in the model as there was no information about the chemical reactions concerning the different types of soil. There is no information present about the subsurface exact contents and data in the PHREEQC databases and literature is very limited to the adsorption of molybdate on iron hydroxides.
The parameters surface area, amount of sites per area and ratio of weak and strong sites are based on

values taken from the literature, and not from the actual site. But as was seen, the values taken from the literature give very high amounts of adsorbed molybdate in the first two scenarios, even higher than in solution. The parameters were lowered, to give values that resonate with more realistic amounts of adsorbed molybdate in scenario 3 and 4. Furthermore, in the model the diffuse double layer model is used, because it has few adjustable parameters and the intrinsic constants used for calculating adsorption are well documented. There has not been modelled with other surface complexation models, as it was not expected that these will provide better results.

5.3 Flow velocities

Flow velocities from the Botlek were taken from MODFLOW and then used in the PHREEQC run file. These flow velocities were taken from 1 particle flow path, and from these velocities the vertical component was taken. These values are rather estimations. However, the only importance of the flow velocities are for the kinetic reactions in the model, thus for the reduction of sulphate to sulphides.

5.4 Layer on the terrain

In 2006, asphalt has been deposited on the terrain, on the unpaved parts. This was done to catch precipitation and preventing it from infiltrating, essentially slowing the transport of molybdenum. This was not modelled. Because the current model has little dependency on time, this is not expected to have any influence on the results.

5.5 Recommendations

A complete answer to the research question beforehand cannot be given. With this is study it is now clear what information is needed to make a model more realistic to the actual situation.
First, to confirm that the described precipitation reactions do occur measurements of the Botlek need to be taken, and check whether these contain molybdenite and/or iron(II)molybdate. If the theories appear to be correct, you need to define a rate law for the precipitation reactions of molybdenite and iron(II)molybdate with rate constants, initial conditions and time steps. This would be the main goal of another research on the behaviour of molybdenum in the subsurface.
It was also seen that the adsorption parameters given by the literature didn't give the desired results. These parameters can be changed according to the literature, but then the results will be based on existing literature. Without actual research data from the Botlek itself it is difficult to underpin these alterations.
To verify the conclusions of this research and to give a groundwater composition more suitable for modelling, the measurements described in table 14 on the next page will need to be done.
It is recommended doing that these additional measurements should be done on the same locations the measurements from MWH regarding sulphate, ferrous iron and molybdate have been done: this would be at the Northern site border, the Site center and the Southern site border. Here the measurements of the concentrations on which the parameterization of the model were taken, so it is suggested to also take the measurements here. Because these site descriptions are still a bit vague, it is suggested to clearly determine where these locations exactly are, i.e. the exact groundwater wells. The measurements of the subsurface composition and the adsorption parameters can be done anywhere on the Climax area, as the subsurface is the same in the entire area. The measurements for molybdate, sulphate, ferrous iron and the cations can also be done at a measuring well with a sample that is already known and provided by MWH. However, it would have to be multiple molybdate measurements at different depths.

Table 14: Recommended measurements

Molybdenite	Verify precipitation reaction
Iron(II)molybdate	Verify precipitation reaction
Pyrite	Verify precipitation reaction
Subsurface composition (e.g. iron oxides, clay particles)	For modelling adsorption behaviour
Molybdate	More measurements for better insight trend
Sulphate	More measurements for better insight trend
Ferrous iron	More measurements for better insight trend
Surface area and surface site density of adsorbents	Lab study, for modelling adsorption behaviour
Cations in groundwater: sodium and calcium	For a correct, charge balanced groundwater composition
Kinetics of the formation of molybdenite and iron(II)molybdate	Lab study, for adequately modelling these kinetic reactions

6.

References

Ali, M., & Dzombak, D. (1996). *Competitive Sorption of Simple Organic Acids and Sulfate on Goethite.* Environmental Science and Technology, 1061-1071.

Allison J.D., B. D.-G. (1991). *MINTEQA2/PRODEFA2, A Geochemical Assessment Model for Environmental Systems: Version 3.0 User's Manual.* U.S. Environmental Protection Agency, 3-91.

Annemieke Marsman, E. v. (2012). *Systeemgrens grondwaterverontreinigingen Rotterdamse Haven.* Utrecht: Deltares.

Barrow, N.J., 1974. *On the displacement of adsorbed anions from soil: 1. Displacement of molybdate by phosphate and by hydroxide.* Soil science, vol. 116, no. 6, p. 423-431.

Bellantoni, A. M. 2014. *The immobilization of molybdenum in the presence of zero valent iron: the role of reductive precipitation versus adsorption.* New Brunswick: Rutgers State University.

Chapelle, F.H., McMahon, P.B., 2008. *Redox Processes and Water Quality of Selected Principal Aquifer Systems.* Ground water, vol. 46, no. 2, p. 259-271.

Chappaz, A., Gobeil, C., Tessier, A. 2008. *Geochemical and anthropogenic enrichment of Mo in sediments from perennially oxic and seasonally anoxic lakes in Eastern Canada.* Geochimica et Cosmochimica Acta, vol. 72, issue 1, p. 170-184.

Goldberg, S., Forster, H. S., and Godfrey, C. L., 1996. *Molybdenum adsorption on oxides, clay minerals, and soils.* Soil Science Society of America Journal, **60**, p. 425-432.

Goldberg, S., Forster, H. S., 1998. *Factors affecting Molybdenum adsorption by soils and minerals.* Soil science, volume 163, issue 2, pp 109-114.

Goldberg, S., 2009. *Influence of soil solution salinity on molybdenum adsorption by soil.* Soil science, vol. 174, p. 9-13.

Goldberg, S., 2010. *Competitive Adsorption of Molybdenum in the Presence of Phosphorus or Sulfur on Gibbsite.* Soil science, volume 175, issue 3, pp 105-110.

IMOA. (1989). *www.imoa.info.* Retrieved 2015, from International Molybdenum Association.

Mettler, S. (2002). *In situ removal from ground water: Fe(II) oxygenation, and precipitation products in a calcareous aquifer.* Zurich: Swiss Federal Institute for Environmental Science and Technology.

Most, E. v. (2012a). *Nader milieukundig bodemonderzoek en geohydrologisch bodemonderzoek aan de Theemsweg 20 te Rotterdam-Botlek.* Zoetermeer: Bk Bodem.

Most, E. v. (2012b). *Jaarlijkse monitoring grondwater Theemsweg 20 te Rotterdam-Botlek.* Zoetermeer: Bk Bodem.

Motta, M.M., Miranda, C.F., 1989. *Molybdate adsorption on Kaolinite, Montmorillonite, and Illite: Constant Capacitance Modeling.* Soil Science Society of America Journal, vol. 53, no. 2, p. 380-385.

MWH B.V. (2014). *Uitvoering nazorgprogramma isolatiemaatregelen 2014.* Amsterdam: MWH.

Parkhurst, D. L., & Appelo, C. (2005). *Description of Input and Examples for PHREEQC* . Retrieved 2015, from USGS: http://wwwbrr.cr.usgs.gov/projects/GWC_coupled/phreeqc/phreeqc3-html/phreeqc3.htm

Rietstra, R., Harmsen, J., 2005. *Geochemie van molybdeen in relatie tot (water)bodemkwaliteit, gewaskwaliteit en diergezondheid*. Wageningen, Alterra, Alterra-rapport 1281. 25 blz.; 1 tab.; 35 ref.

Stollenwerk, K., 1995. *Modeling the effects of variable groundwater chemistry on adsorption of molybdate*. Water Resources Research , volume 31, no 2, pages 347-357.

Stumm, W., & Morgan, J. J. (1996). *Aquatic Chemistry*. New York: John Wiley & Sons.

Vacchina, V. (2014). *Molybdate speciation in waters*. Amsterdam-Duivendrecht: Omegam Laboratoria.

Verbinnen, B., Block, C., Hannes, D., Lievens, P., Vaclavikova, M., Stefusova, K., Gallios, G. Vandecasteele, C., 2012. *Removal of Molybdate Anions from Water by Adsorption on Zeolite-Supported Magnetite*. Water Environment Research, 84, 753-760.

Vermeulen, P.T.M., 2006. *Model-Reduced Inverse Modeling*. Ph.D. thesis Delft University of Technology - with ref. - with summary in Dutch. ISBN-10: 90-9020536-5. ISBN-13: 978-90-9020536-6

Xu, N., Christodoulatos, C., Braida, W., 2005. *Adsorption of molybdate and tetrathiomolybdate onto pyrite and goethite: Effect of pH and competitive anions*. Chemosphere, volume 62, issue 10, pp 1726-1735.

Appendix A – measurements UT2A

Ultra Traces Analyses Aquitaine

Hélioparc Pau Pyrénées
2, avenue du Président Angot
F-64053 PAU Cedex 9
Tél. : +33-(0)5-40-17-51-80
Fax : +33-(0)5-40-17-51-90
e-mail : ut2a@univ-pau.fr
www.ut2a.fr

Analysis report
P14-097

Title : Molybdate speciation in waters

Company : Omegam Laboratoria
Contact : Franka KNIP
Adress : H.J.E. Wenckebachweg 120

Postal Code: 1114AD
Town: Amsterdam-Duivendrecht

E-mail : f.knip@omegam.nl

Purchase order : according to financial proposal D14-026
Reception data : January 31th 2014
Number of samples : 4
Sample type : water
Responsible of analysis : Véronique VACCHINA
Operators : Véronique VACCHINA
Analysis date : February 13th and 17th 2014

Method : Internal

General comments :

The results given in this report are obtained from a sample provided by the test. This document cancels and replaces all the previous report sent with the same reference. Any copy even partial has to be requested to the authors.

Date : February 17th 2014 || ***Writer*** : Véronique VACCHINA || ***Approver*** : Fabienne SEBY

Accounting Service
162 avenue Albert Schweitzer
CS60040 - 33608 PESSAC
n° SIRET : 77558634000041

Project : 478762 Sample number : 0546444 1015-1-1 gefiltreerd bc B54663563 Order number : UA140122 Sampling date : 28/01/2014						
Parameters	**Techniques**	**Result.**	**Uncert.**	**QL**	**Unit**	**Comment**
MoO_4^{2-}	HPLC – ICP MS	1.7	0.1	1	µg Mo/L	

Project : 478762 Sample number : 0546445 1015-1-1 ongefiltreerd bc B54663574 Order number : UA140122 Sampling date : 28/01/2014						
Parameters	**Techniques**	**Result.**	**Uncert.**	**QL**	**Unit**	**Comment**
MoO_4^{2-}	HPLC – ICP MS	43.9	0.6	1	µg Mo/L	

Project : 478762 Sample number : 0546540 3401-1-1 gefiltreerd bc B54663631 Order number : UA140122 Sampling date : 28/01/2014						
Parameters	**Techniques**	**Result.**	**Uncert.**	**QL**	**Unit**	**Comment**
MoO_4^{2-}	HPLC – ICP MS	90	1	1	µg Mo/L	

Project : 478762 Sample number : 0546541 3401-1-1 ongefiltreerd bc B54663620 Order number : UA140122 Sampling date : 28/01/2014						
Parameters	**Techniques**	**Result.**	**Uncert.**	**QL**	**Unit**	**Comment**
MoO_4^{2-}	HPLC – ICP MS	94	1	1	µg Mo/L	

QL : Quantification Limit
The uncertainty is expressed as 2 times the standard deviation (95% confidence level)

UT2A - Hélioparc Pau Pyrénées - 2, avenue du Président Angot - F-64053 PAU Cedex 9
Tél. : +33-(0)5-40-17-51-80 | Fax : +33-(0)5-40-17-51-90 | e-mail : ut2a@univ-pau.fr | www.ut2a.fr
ADERA PESSAC 162 avenue Albert Schweitzer - BP 196 - 33608 PESSAC Tél. : +33-(0)5-56-15-11-57 Fax : +33-(0)-5-56-15-11-60

Ultra Traces Analyses Aquitaine

Hélioparc Pau Pyrénées
2, avenue du Président Angot
F-64053 PAU Cedex 9
Tél. : +33-(0)5-40-17-51-80
Fax : +33-(0)5-40-17-51-90
e-mail : ut2a@univ-pau.fr
www.ut2a.fr

Analysis report
P14-098

Title : Molybdate speciation in waters

Company : Omegam Laboratoria
Contact : Franka KNIP
Adress : H.J.E. Wenckebachweg 120

Postal Code: 1114AD
Town: Amsterdam-Duivendrecht

E-mail : f.knip@omegam.nl

Purchase order : according to financial proposal D14-026
Reception data : January 31th 2014
Number of samples : 2
Sample type : water
Responsible of analysis : Véronique VACCHINA
Operators : Véronique VACCHINA
Analysis date : February 17th 2014

Method : internal

General comments :

The results given in this report are obtained from a sample provided by the test. This document cancels and replaces all the previous report sent with the same reference. Any copy even partial has to be requested to the authors.

Date : February 17th 2014 || ***Writer*** : Véronique VACCHINA || ***Approver*** : Fabienne SEBY

1/2

Accounitng Service
162 avenue Albert Schweitzer
CS60040 - 33608 PESSAC
n° SIRET : 77558634000041

Project : 478748 *Sample number : 0546393 607R-1-1 gefiltreerd bc B54663620* *Order number : UA140126* *Sampling date : 29/01/2014*						
Parameters	**Techniques**	**Result.**	**Uncert.**	**QL**	**Unit**	**Comment**
MoO_4^{2-}	HPLC – ICP MS	1335	26	1	µg Mo/L	

Project : 478748 *Sample number : 0546393 607R-1-1 ongefiltreerd bc B54663620* *Order number : UA140126* *Sampling date : 29/01/2014*						
Parameters	**Techniques**	**Result.**	**Uncert.**	**QL**	**Unit**	**Comment**
MoO_4^{2-}	HPLC – ICP MS	1339	11	1	µg Mo/L	

P14-098

QL : Quantification Limit
The uncertainty is expressed as 2 times the standard deviation (95% confidence level)

UT2A - Hélioparc Pau Pyrénées - 2, avenue du Président Angot - F-64053 PAU Cedex 9
Tél. : +33-(0)5-40-17-51-80 | Fax : +33-(0)5-40-17-51-90 | e-mail : ut2a@univ-pau.fr | www.ut2a.fr
ADERA PESSAC 162 avenue Albert Schweitzer - BP 196 - 33608 PESSAC Tél. : +33-(0)5-56-15-11-57 Fax : +33-(0)-5-56-15-11-60

Appendix B – PHREEQC model

```
#DATABASE C:\Program Files (x86)\USGS\Phreeqc Interactive 3.1.7-9213\database\wateq4f.dat
TITLE 10 cm soil column                                                    # Database: wateq


######EXTENDED DATABASE######


SURFACE_SPECIES
        Hfo_sOH + MoO4-2 + H+ = Hfo_sMoO4- + H2O
                log_k           9.5
        Hfo_sOH + MoO4-2 = Hfo_sOHMoO4-2
                log_k           2.4
        Hfo_wOH + MoO4-2 + H+ = Hfo_wMoO4- + H2O
                log_k           9.5
        Hfo_wOH + MoO4-2 = Hfo_wOHMoO4-2
                log_k           2.4
SOLUTION_MASTER_SPECIES
Fe_di           Fe_di+2   0.0    Fe_di          55.847
Fe_tri          Fe_tri+3  0.0    Fe_tri         55.847
Mo                        MoO4-2    0.0    Mo                        95.94
SOLUTION_SPECIES
        MoO4-2 + H+ = HMoO4-
            log_k           4.2988
           delta_h          20 kJ
    MoO4-2 + 2H+ = H2MoO4
            log_k           8.1636
            delta_h         -26 kJ
    7MoO4-2 + 8H+ = Mo7O24-6 + 4H2O
            log_k           52.99
            delta_h         -228        kJ
    7MoO4-2 + 9H+ = HMo7O24-5 + 4H2O
            log_k           59.3768
            delta_h         -218        kJ
        7MoO4-2 + 10H+ = H2Mo7O24-4 + 4H2O
            log_k           64.159
            delta_h         -215        kJ
        7MoO4-2 + 11H+ = H3Mo7O24-3 + 4H2O
            log_k           67.405
            delta_h         -217        kJ
        MoO4-2 = MoO4-2
                log_k           0.0
        Fe_di+2 = Fe_di+2
          log_k           0.0
        Fe_tri+3 = Fe_tri+3
          log_k       0.0
    H2O + 0.01e- = H2O-0.01
          log_k             -9
#
# Fe+2 species
```

```
#
Fe_di+2 + H2O = Fe_diOH+ + H+
      log_k   -9.5
      delta_h 13.20   kcal
#
#... and also other Fe+2 species
#
Fe_di+2 + Cl- = Fe_diCl+
      log_k   0.14
Fe_di+2 + CO3-2 = Fe_diCO3
      log_k   4.38
Fe_di+2 + HCO3- = Fe_diHCO3+
      log_k   2.0
Fe_di+2 + SO4-2 = Fe_diSO4
      log_k   2.25
Fe_di+2 + HSO4- = Fe_diHSO4+
      log_k   1.08
Fe_di+2 + 2HS- = Fe_di(HS)2
      log_k   8.95
Fe_di+2 + 3HS- = Fe_di(HS)3-
      log_k   10.987
#
# Fe+3 species
#
Fe_tri+3 + H2O = Fe_triOH+2 + H+
      log_k   -2.19
      delta_h 10.4    kcal
#
#... and also other Fe+3 species
#
Fe_tri+3 + 2 H2O = Fe_tri(OH)2+ + 2 H+
      log_k   -5.67
      delta_h 17.1    kcal
Fe_tri+3 + 3 H2O = Fe_tri(OH)3 + 3 H+
      log_k   -12.56
      delta_h 24.8    kcal
Fe_tri+3 + 4 H2O = Fe_tri(OH)4- + 4 H+
      log_k   -21.6
      delta_h 31.9    kcal
2 Fe_tri+3 + 2 H2O = Fe_tri2(OH)2+4 + 2 H+
      log_k   -2.95
      delta_h 13.5    kcal
3 Fe_tri+3 + 4 H2O = Fe_tri3(OH)4+5 + 4 H+
      log_k   -6.3
      delta_h 14.3    kcal
Fe_tri+3 + Cl- = Fe_triCl+2
      log_k   1.48
      delta_h 5.6     kcal
Fe_tri+3 + 2 Cl- = Fe_triCl2+
      log_k   2.13
Fe_tri+3 + 3 Cl- = Fe_triCl3
```

```
    log_k   1.13
Fe_tri+3 + SO4-2 = Fe_triSO4+
    log_k   4.04
    delta_h 3.91    kcal
Fe_tri+3 + HSO4- = Fe_triHSO4+2
    log_k   2.48
Fe_tri+3 + 2 SO4-2 = Fe_tri(SO4)2-
    log_k   5.38
    delta_h 4.60    kcal
PHASES
Goethite
    Fe_triOOH + 3 H+ = Fe_tri+3 + 2 H2O
    log_k   -1.0
pH_Fix
        H+ = H+;
        log_k 0
Mackinawite
    Fe_diS + H+ = Fe_di+2 + HS-
    log_k   -4.648
Pyrite
    Fe_diS2 + 2H+ + 2e- = Fe_di+2 + 2HS-
    log_k   -18.479
Fe_MoO4
        Fe_diMoO4 = MoO4-2 + Fe_di+2
        log_k   -10.091
MoS2
        MoS2 + 4H2O = MoO4-2 + 6H+ + 2HS- + 2e-
        log_k   -59.27


######MINERALS AND SURFACES######


EQUILIBRIUM_PHASES 1-501
        Goethite                    0 0.0674
        MoS2                0 0
        Fe_MoO4                     0 0
        Pyrite              0 0
        Mackinawite         0 0
SURFACE 1-501
        Hfo_wOH Goethite    0.27 17800
        Hfo_sOH Goethite    0.0066654


######INFILTRATING SOLUTION######


SOLUTION 0
        units ppm
        pH                  6.86
        Mo                  15
```

```
        Fe_di       10.25
        Alkalinity      260 as HCO3-
        Cl              136
        S(6)            400 as SO4-2
        Na              200
        Ca              150


######INITIAL COLUMN CONDITIONS######


SOLUTION 1-501
        units ppm
        pH              6.86
        Fe_di       10.25
        Alkalinity      175 as HCO3-
        Cl              50
        Na              50
        Ca              40
END


######RATES AND KINETICS######


USE Solution 1
KINETICS 1-501
        Organic_C
        -formula                CH2O
        -m                      0.08
        -m0                     0.08
        -tol            1.e-8
        -steps          100 second
        -runge_kutta    6
        -cvode          false
        -bad_step_max           500
RATES
Organic_C
 -start
  1  rem     Additive Monod kinetics
  2  rem     Electron acceptors: SO4
  10 if (m <= 0) then goto 200
  20  mSO4 = tot("S(6)")
  30   rate = 3e-10*mSO4/(1.e-3 + mSO4)
  40  moles = rate * m * (m/m0) * time
  50 if (moles > m) then moles = m
  200 save moles
 -end
END
```

```
######TRANSPORT######


TRANSPORT
        -cells                  501
        -shifts                 730
        -time_step              2074645
        -flow_direction                 forward
        -boundary_conditions    flux flux
        -lengths                        50*0.1 110*0.045418145 145*0.041443124
181*0.049847514 15*0.334017966
#       -dispersivity           501*0.50
#       -punch_cells            10
        -punch_frequency        730

######OUTPUT FILE CONTENT######


SELECTED_OUTPUT
        -file                   Concentrations_correct_model.out
        -reset                  false
        -pH                             true
        -step                   true
        -high_precision                 true
        -equilibrium_phases     MoS2 Fe_MoO4 Pyrite Mackinawite
USER_PUNCH
        -heading Years Depth S(6)_mg S(-2)_mg Fe_di_ug Fe_tri_ug HCO3_mg Cl_mg Ca_mg
MoO4-2_ug Sorbed_MoO4-2 Tot_Mo
        10 PUNCH (TOTAL_TIME)/31536000
        20 PUNCH -(DIST)
        30 PUNCH TOT("S(6)")*96.06*1000
        40 PUNCH TOT("S(-2)")*32.064*1000
        50 PUNCH TOT("Fe_di")*55.845*1000000
        60 PUNCH TOT("Fe_tri")*55.845*1000000
        70 PUNCH MOL("HCO3-")*50.05*1000
        80 PUNCH TOT("Cl")*35.45*1000
        90 PUNCH TOT("Ca")*40.078*1000
        100 PUNCH TOT("Mo")*95.9576*1000000
        110 PUNCH SURF("Mo", "Hfo")*95.9576*1000000
        120 PUNCH (TOT("Mo")*95.9576*1000000)+(SURF("Mo", "Hfo")*95.9576*1000000)

END
```